Sandra Huber, BSc

Pigment Epithelium Derived Factor in lipid metabolism

MASTER'S THESIS

To achieve the university degree of

Master of Science

Master's degree programme: Biochemistry and Molecular Biomedical Sciences

submitted to

Graz University of Technology

Supervisor

Priv.-Doz. Mag. Dr. Martina Schweiger

Institute of Molecular Biosciences

Graz, September 2019

AFFIDAVIT

I declare that I have authored this thesis independently, that I have not used other than the declared sources/resources, and that I have explicitly indicated all material which has been quoted either literally or by content from the sources used.

The text document uploaded to TUGRAZonline is identical to the present master's thesis dissertation.

Date	Signature

Danksagung

Zunächst möchte ich mich an dieser Stelle bei all denjenigen bedanken, die mich während der Masterarbeit im Labor unterstützt haben und mich immer wieder motiviert haben.

Ich möchte mich besonders bei Martina Schweiger für ihre herzliche und informative Betreuung während der gesamten Masterarbeit bedanken. Durch ihre Unterstützung und Expertise konnte ich mich immer an sie wenden, gemeinsame Überlegungen anstellen und mich dadurch weiterentwickeln.

Ebenfalls möchte ich mich bei meinen Laborkollegen Pia, Isabella, Ursula und Sandra bedanken, die mich zu Beginn der Masterarbeit sehr unterstützt haben. Des Weiteren möchte ich mich beim gesamten Labor stockwerkübergreifend für die gute Zusammenarbeit und das angenehme Arbeitsklima bedanken.

Bei meinen Studienkollegen/Innen möchte ich mich für die gemeinsame Studienzeit bedanken. Ohne die gemeinsamen Unternehmungen wäre es in Graz sicher nicht so lustig geworden.

Zusätzlich möchte ich mich noch bei meinen Freunden aus Salzburg und Ried im Innkreis bedanken, die mich den Studienstress während unserer Treffen vergessen lassen haben.
Mein größter Dank gilt meiner Familie und besonders meinen Eltern, die immer für mich da waren und mir dieses Studium ermöglicht haben. Ein spezieller Dank gilt meinem Freund Christoph, der mir immer wieder seelische Unterstützung gegeben hat.

Abstract

Pigment epithelium derived factor (PEDF), encoded by the SERPINF1 gene, is a multifunctional glycoprotein of 50 kDa and highly abundant in the plasma. It belongs to the serine protease inhibitor family and was first discovered as a neurotrophic factor secreted by retinal pigment epithelial cells in humans. In addition to this function, PEDF also plays a role as an anti-tumour agent by inducing apoptosis and inhibiting angiogenesis. Moreover, PEDF has been associated with type 2 diabetes and insulin resistance indicating a metabolic role of the protein. In hepatocytes, PEDF is thought to have a pro-lipolytic function by binding to the enzyme adipose triglyceride lipase (ATGL). In cornea, PEDF binds to ATGL on the plasma membrane and stimulates its phospholipase A2 activity. Recent studies showed that PEDF protects from obesity and metabolic disorders in mice fed a high fat diet. However, so far, it is not clear how PEDF regulates lipid metabolism. Therefore, the aim of my master thesis was to investigate how PEDF exerts its effect on lipid metabolism. Therefore, I characterized mice globally lacking PEDF. Moreover, I performed cell culture and in vitro studies to study PEDF in lipolysis and cell differentiation.

PEDF deficient animals (KO) fed a chow diet did not differ from their wild-type (WT) littermates with regard to body and tissue weights and liver energy stores. Plasma lipid and glucose parameters were not different between PEDF-KO and their WT littermates, in the fed, fasted, or cold exposed state. Addition of recombinant PEDF as well as lentiviral PEDF overexpression slightly increased lipolysis of adipocytes. However, in vitro TG hydrolase activity remained unaffected by PEDF, excluding a direct effect on ATGL activity. In addition, PEDF had no influence on adipocyte differentiation and did not affect ATGL protein expression.

Taken together in my thesis I found that PEDF deficiency does not affect lipid metabolism in mice on a chow diet or in cultured adipocytes. Overexpression of PEDF, however slightly increases lipolysis. More studies are needed to clarify the role of PEDF in lipid metabolism.

Zusammenfassung

Pigment epithelium derived factor (PEDF), wird vom SERPINF1 Gen kodiert und ist ein multifunktionales Glykoprotein mit einer Größe von 50 kDa. PEDF gehört zur Familie der Serin-Protease-Inhibitoren und wurde als neurotropher Faktor entdeckt, der von retinalen Pigmentepithelzellen im Menschen sekretiert wird. Neben dieser Funktion spielt PEDF in der Apoptose und der Angiogenese eine Rolle. Darüber hinaus wurde PEDF mit Typ-2-Diabetes und Insulinresistenz assoziiert, was auf eine metabolische Rolle hinweist. In Hepatozyten soll PEDF einen pro-lipolytische Effekt haben, indem es an das Enzym Adipose triglyceride lipase (ATGL) bindet. In der Hornhaut bindet PEDF an ATGL auf der Plasmamembran und stimuliert dessen Phospholipase A2-Aktivität. Aktuelle Studien zeigten, dass PEDF, Mäuse mit einer fettreichen Ernährung, vor Fettleibigkeit und Stoffwechselstörungen schützte. Bisher ist jedoch unklar, wie PEDF den Fettstoffwechsel reguliert. Daher war das Ziel meiner Masterarbeit zu untersuchen, wie PEDF auf den Fettstoffwechsel wirkt. Dafür habe ich Mäuse charakterisiert, denen global PEDF fehlt. Darüber hinaus führte ich Zellkultur- und In-vitro-Studien durch um PEDFs Effekt in der Lipolyse sowie der Zelldifferenzierung zu untersuchen.

PEDF defiziente (KO) Tiere, die mit Chow Diät gefüttert wurden, wiesen keinen Unterschied in Bezug auf das Körper- und Gewebegewicht sowie die Leberenergiespeicher zu ihren Wildtyp-(WT) Wurfgeschwistern auf. Des Weiteren gab es auch keine Unterschiede in den Lipid- und Glucose-Parametern im Plasma zwischen PEDF-KO und ihren WT-Wurfgeschwistern im gefütterten, nüchternen oder Kälte-exponierten Zustand. Die Zugabe von rekombinantem PEDF sowie die Überexpression von lentiviralem PEDF führte zu einem kleinen Anstieg der Lipolyse von Adipozyten. Die In-vitro-TG-Hydrolase Aktivität blieb jedoch durch PEDF unverändert, wodurch ein direkter Effekt auf die ATGL-Aktivität ausgeschlossen werden kann. Darüber hinaus hatte PEDF keinen Einfluss auf die Adipozyten-Differenzierung sowie auf die Proteinexpression von ATGL.

Zusammengefasst stellte ich in meiner Arbeit fest, dass ein PEDF-Mangel den Fettstoffwechsel bei Mäusen, die eine Chow-Diät erhielten, oder bei kultivierten Adipozyten nicht beeinflusst. Jedoch führte die Überexpression von PEDF zu einer leicht erhöhten Lipolyse. Weitere Studien sind erforderlich, um die Rolle von PEDF im Fettstoffwechsel zu klären.

Table of content

1. Introduction

1.1 Ingestion and storage of lipids

After a meal, dietary fat in form of triacylglycerol (TG) is already partially degraded by lipolytic enzymes in the mouth (linguinal lipase), stomach and intestine (pancreatic lipase) to monoglycerides (MG) and fatty acids (FA). In the mucosal cells of the intestine FA and MG are reesterified to TG, packed into lipoprotein particles (chylomicrons) and released into the lymph and subsequently the blood. From the blood dietary lipids are cleaved by the activity of lipoprotein lipase (LPL). LPL hydrolyses TG within lipoproteins at the capillary endothel of most tissues. The released FA are taken up and either oxidized or stored as TG. Adipose tissue (AT) takes up any surplus of energy and stores it for less profitable times (Voet et al. 2008, Rassow et al. 2012).

AT is a complex, endocrine organ consisting of adipocytes, extracellular matrix, neurons, stromal vascular- and immune cells (Kershaw et al. 2004). It is capable of synthesizing and secreting various hormones and therefore influences whole body metabolism. Moreover, AT is a metabolically dynamic organ which acts as main energy reservoir. It takes up dietary lipids and releases them back into the bloodstream to provide energy for oxidative tissues upon demand (Coelho et al. 2012).

There are two types of AT with different characteristics, white and brown AT. Brown adipocytes are small and multilocular compared to white adipocytes and have a high mitochondrial density (Xu et al. 2019). The functional role of brown adipose tissue (BAT) is to provide heat by thermogenesis. Thermogenesis is switched on by the expression of the “uncoupling protein 1” (UCP1) which uncouples the proton gradient in mitochondria from ATP synthesis resulting in heat production. UCP1 is unique for BAT and is located in the inner mitochondrial membrane (Bal et al. 2017, Klingenspor et al. 2003). Besides body weight homeostasis and immunity, white adipose tissue (WAT) is also important for coagulation, angiogenesis, reproduction as well as glucose and lipid metabolism (Coelho et al. 2012). WAT mass is closely associated with metabolic disorders and obesity, whereas BAT has been shown to counteract obesity (Xu et al. 2019).

1.2 Lipolysis

Lipolysis is a biochemical process whereby TG are hydrolysed to FA and glycerol. It is executed by three different lipases and takes place on the surface of intracellular lipid droplets. The first step is the hydrolysis of TG to diacylglycerols (DG) by adipose triglyceride lipase (ATGL) (Duncan et al. 2007). In the second step hormone-sensitive lipase (HSL) hydrolyses DG to MG. Finally, monoglyceride lipase (MGL) degrades MG to FA and glycerol (Lass et al. 2011).

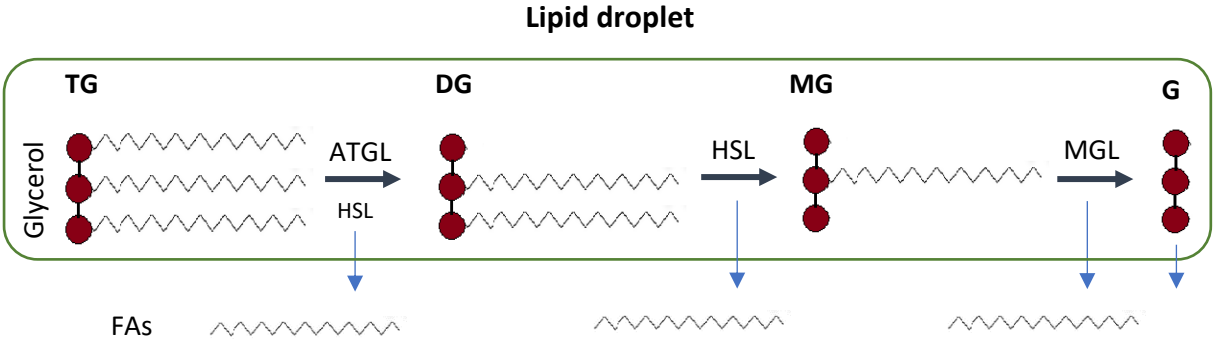

Figure 1.1: Schematic illustration of lipolysis. TG are hydrolysed by the enzymes ATGL, HSL and MGL resulting in the release of FA and glycerol.

1.2.1 Enzymes involved in lipolysis

ATGL, also called PNPLA2, Desnutrin, TTS2.2, iPLA2ζ, is a 54 kDa protein mostly expressed in WAT and BAT (Duncan et al. 2007, Chakrabarti et al. 2013). The enzyme is also detectable in in other tissues such as testis, liver, cardiac- and skeletal muscle. ATGL contains a patatin domain (PD) at the N-terminus, which is characterized by a conserved serine and aspartate forming the catalytic site as well as an α/β-hydrolase fold and a glycine rich region (Duncan et al. 2007). ATGL is well conserved and expressed in other species such as fly, rat and plants. Human and murine ATGL exhibit a size of 504 and 485 amino acids (aa), respectively and share 84% aa identity (Lass et al. 2011). The PD of human and murine ATGL share a sequence identity of >95% (Zechner et al. 2009).

The crucial role of ATGL in maintaining energy homeostasis became evident by the phenotype of the ATGL deficient mouse model (Zimmermann et al. 2009). Knockout of ATGL in mice results in reduced lipolytic activity in AT as well as in testis, liver, cardiac- and skeletal muscle (Haemmerle et al. 2006). In ectopic tissues, absence of ATGL results in increased ac-

cumulation of TG leading to cardiac failure and premature death in mice. In humans, ATGL deficiency is called Neutral lipid storage disease with myopathy. Patients with this disease exhibit TG accumulation in leucocytes as well as cardiac- and skeletal muscle myopathy but do not develop insulin resistance (IR) (Zimmermann et al. 2009).

HSL consists of 775 aa in human and 759 aa in mice (Haemmerle et al. 2002, Li et al. 1994). HSL hydrolyses TG, DG, MG as well as cholesteryl esters (CE) and retinyl esters (RE). However, it has a 10-fold higher specificity for DG compared to the other substrates (Haemmerle et al. 2002). HSL contains a GXSXG motif in the active site but has no further homology to other lipases (Lass et al. 2011). HSL deficiency in mice leads to an accumulation of DG in AT, testis, and cardiac- and skeletal muscle (Haemmerle et al. 2002).

MGL is a 33 kDa protein hydrolysing MG to glycerol and FA. MGL consists of 302 aa and has a catalytic triad consisting of Asp-239, Ser-122, and His-269. Regarding the serine residue, the motif of the catalytic site is GXSXG (Duncan et al. 2007). MGL deficiency leads to altered lipid metabolism (Vujic et al. 2017). Furthermore, MGL-KO mice fed a high fat diet (HFD) were protected from liver steatosis and IR indicating that MGL plays a major role in the development of metabolic disorders (Yoshida et al. 2019).

1.2.2 Regulation of lipolysis by proteins and hormones

Lipolysis is nutritionally regulated. During times of nutrient deprivation, catecholamines and glucocorticoids stimulate lipolysis (Jaworski K. et al. 2007). Catecholamines activate lipolysis by binding to β-adrenergic receptors (AR) (Langin D. 2006). Binding of catecholamines to β-AR leads to dissociation of the activatory subunit and activation of adenylate cyclase (AC). AC catalyses the production of cyclic adenosine monophosphate (cAMP) from adenosine triphosphate (ATP) which activates protein kinase A (PKA), a central enzyme in lipid metabolism. PKA phosphorylates HSL and perilipin, the most abundant lipid droplet associated protein. Phosphorylation of these two proteins increases HSL activity (Jaworski K. et al. 2007). ATGL activity is indirectly activated by the phosphorylation of perilipin. Perilipin binds to and sequesters the activator of ATGL comparative gene identification protein- 58 (CGI-58). Upon phosphorylation of perilipin, CGI-58 is released and binds to and activates ATGL (Granneman et al. 2007, Lass et al. 2006).

Lipolysis is suppressed by the feeding hormone insulin (Jaworski K. et al. 2007). Binding of insulin to its receptor induces conformational change leading to autophosphorylation. Thereby, the receptor is activated and further activates insulin receptor substrate (IRS) by phosphorylation of tyrosine residues. This in turn leads to the association of IRS with phosphatidylinositol 3-kinase (PI3)/Akt and the phosphorylation of phosphodiesterase 3B (PDE3B) resulting in degradation of cAMP. This inactivates PKA, which leads to reduced phosphorylation of HSL and perilipin (Jaworski K. et al. 2007, https://www.abcam.com/pathways/overview-of-insulin-signaling-pathways, Accessed September 17.2019).

Insulin also inhibits lipolysis by reducing ATGL transcription. Recent studies indicate that forkhead transkription factor 1 (FoxO1) is an important regulator of ATGL expression. When insulin binds to the insulin receptor, FoxO1 is phosphorylated and inactivated. This suppresses ATGL expression (Chakrabarti et al. 2011). Insulin also activates mTORC1. mTORC1 activates early growth response protein 1 (Egr1), which leads to the inhibition of ATGL transcription and lipolysis (Chakrabarti et al. 2013). Regulation of lipolysis by catecholamines and insulin is depicted in Figure 1.2.

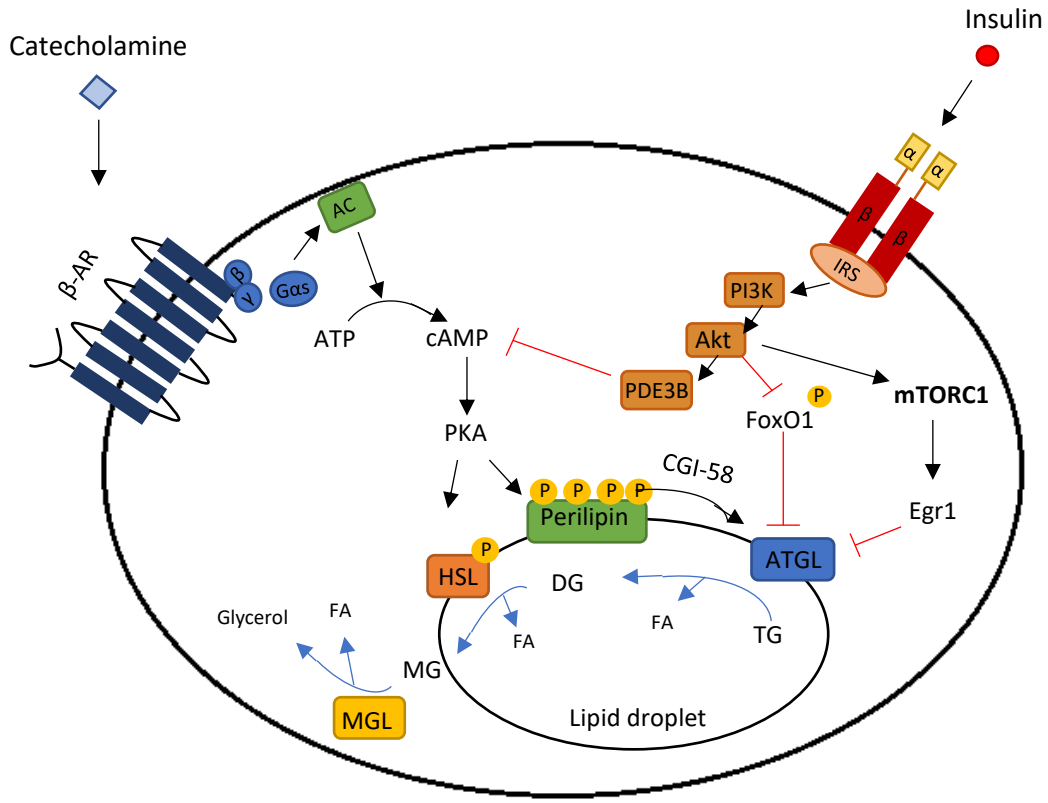

Figure 1.2: Regulation of lipolysis. In this figure, two pathways are presented. The first pathway is binding of catecholamines which leads to an activation of AC resulting in increased levels of intracellular cAMP. If cAMP is increased, PKA is activated leading to phosphorylation of HSL and Perilipin. This is responsible for enhanced lipolysis. The other pathway is binding of insulin to its receptor leading to the activation of PI3K and Akt, which in turn activates PDE3B. This lowers intracellular cAMP as well as PKA activity resulting in decreased lipolysis. Akt affects ATGL activity by inhibition of FoxO1 or activation of mTORC1.

1.3 Obesity and Insulin resistance

Obesity is characterized by an excessive growth of AT depots. This results from hyperplasia and hypertrophy of adipocytes, in a depot-dependent manner (Hardy et al. 2014). Besides affecting social-, mental-, and spiritual health, obesity is associated with the development of type 2 diabetes, cardiovascular diseases, or cancer (Djalalinia et al. 2015). Obesity leads to IR, causing increased insulin secretion from pancreatic β-cells, hyperinsulinemia, finally leading to pancreatic dysfunction (Guo et al. 2014). IR is determined by a reduced response of a specific cell to insulin. IR causes an impaired blood glucose reducing effect mediated by circulating or injected insulin in the whole body (Czech et al. 2017). One of the major contributors to IR in obesity is the increased release of FA from the expanded AT. These FA are targeted to ectopic tissues where they interfere with insulin signalling (Hardy et al. 2014).

1.4 PEDF

Pigment epithelium derived factor (PEDF) is a 50 kDa glycoprotein released by pigment epithelial cells (Notari et al. 2006, Carnagarin et al. 2015). PEDF is encoded by the SERPINF1 gene and composed of 418 aa. PEDF is a non-inhibitory serine protease inhibitor with a protease sensitive reactive central loop (RCL) at the C-terminus. Hence, it harbours a typical motif for serine protease inhibitors but does not inhibit those enzymes. This might be due to the RCL, which does not change conformation upon cleavage (Carnagarin et al. 2015). In humans, PEDF concentration in plasma is approx. 5 µg/ml. This highly abundant plasma protein is secreted by several organs such as liver, AT, lung, bone, kidney, eye and pancreas (He et al. 2015). PEDF was identified to have neurotrophic, -protective, antiangiogenic, and proapoptotic functions. PEDFs antitumor effects are due to its antiangiogenic function as well as its ability to induce apoptosis (Fernandez-Garcia et al. 2007). Another important function of PEDF is the suppression of tumour cell migration by its antimetastatic activity (Becerra & Notario. 2013).

Based on its neurotrophic function, Huang M. et al. (2018) showed that PEDFs serum levels decrease with age and even more with Alzheimer's disease, suggesting that PEDF-deficiency plays a crucial role in the development of such a disease.

Moreover, in previous studies vascular endothelial growth factor (VEGF) has been shown to be important in ocular neovascularization in ischemic retinopathies. PEDF inhibits not only VEGF-induced retinal endothelial cell growth but also neovascularization and migration (Duh et al. 2002).

However, over the last two decades, PEDF has become a popular protein in studying metabolism. With regard to lipid metabolism PEDF has been shown to affect adipogenesis and lipolysis, and hence is implicated in the development of obesity and IR (Borg et al. 2011, Wang et al. 2009). PEDF has an inhibitory effect on adipogenesis partly by blocking MAPK/ERK pathway in 3T3-L1 preadipocytes. Additionally, protein and mRNA levels of PEDF are highly expressed in preadipocytes, leading to an inhibition of differentiation and lipid accumulation, whereas in adipocytes, PEDF is strongly decreased (Wang et al. 2009).

Controversial studies have been published on the effect of PEDF on lipolysis. Niyogi et al. (2019) investigated the role of PEDF in regulating hepatic lipid accumulation by ATGL. They demonstrated that PEDF causes degradation of ATGL by COP1 in the nucleus. Another study

claimed that PEDF binds to a PEDF receptor, which is identical to ATGL. Binding of PEDF to ATGL activates its phospholipase A2 (PLA) activity (Notari et al. 2006).

Borg et al. (2011) showed that PEDF enhances basal ATGL-mediated lipolysis in AT but does not affect lipolysis upon β-adrenergic stimulation. Other studies indicate that PEDF reduces ATGL protein content by proteasomal degradation, and thereby reduces lipolytic activity (Dai et al. 2013a). The phenotype of PEDF deficient mice indicate a crucial role of PEDF in liver lipid metabolism. PEDF-KO mice have increased TG content in hepatocytes. This might be due to an impaired TG-hydrolase activity (Chung et al. 2008).

In humans, circulating PEDF is associated with several metabolic disorders including obesity, type 2 diabetes and metabolic syndrome (Huang K. et al. 2018a). Regarding obese rodent models, PEDF expression in adipocytes as well as serum levels are increased (Crowe et al. 2009). Previous studies revealed that PEDF participates in metabolic inflammation promoting IR. It is suggested that elevated PEDF increases ATGL mediated lipolysis in adipocytes and leads to an increased flux to oxidative tissues. This may cause ectopic lipid storage and IR (Huang K. et al. 2018a). In figure 1.3, previously described functions of PEDF are summarized.

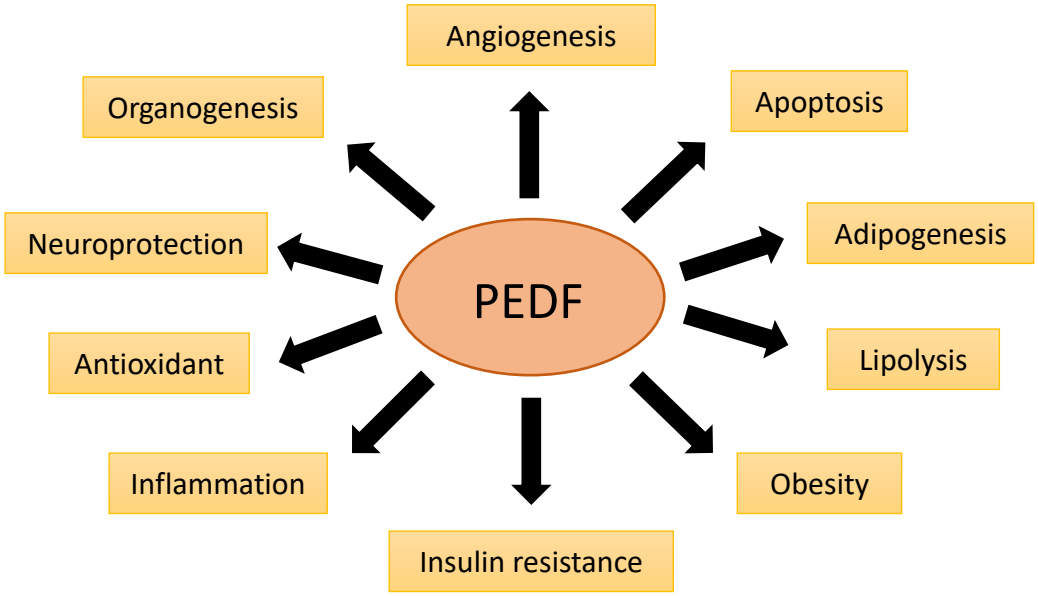

Figure 1.3: PEDF is a multifunctional protein. It shows anti-tumour effects (pro-apoptosis, pro-inflammatory, anti-angiogenic). It participates in organogenesis and is involved in neuroprotection. Also, it has an antioxidant activity. Predominantly, PEDF is involved in lipid metabolism including adipogenesis, lipolysis, obesity and IR.

1.5 Aim of this project

PEDF has been shown to affect systemic lipid metabolism by regulating the activity of ATGL in AT and the liver (Notari et al. 2006, Chung et al. 2008). However, to date is not known how PEDF exerts its pro- or anti-lipolytic function. Hence, the aim of my master thesis was to investigate the role of PEDF in lipid metabolism.

To examine the role of PEDF in lipid metabolism, I overexpressed and purified recombinant PEDF. Using different adipocyte cell culture models, I elucidated the role of PEDF in adipocyte differentiation. Moreover, I investigated whether deficiency of PEDF, the addition of recombinant PEDF or addition of conditioned media of PEDF overexpressing cells affect adipocyte and AT lipolysis, respectively.

To elucidate the feeding-fasting regulation of PEDF in WT and PEDF-KO mice, blood glucose and plasma parameters were determined. Furthermore, I analysed PEDF and ATGL protein and mRNA expression in WT and PEDF-KO tissues. Due to the prominent role of PEDF in liver lipid metabolism, glycogen as well as lipid composition of WT and PEDF-KO livers were determined.

In order to investigate the role of PEDF in thermogenesis, a cold exposure experiment was performed. Therefore, mice were placed in a chamber at a constant temperature of 5°C. Then, body weight, body temperature and blood glucose content as well as plasma parameters were examined.

2. Material

2.1 Buffer and solutions

Solution A (pH 7.0)

- 250 mM Sucrose
- 1 mM Ethylenediaminetetra-acetic acid (EDTA)
- 1 mM Dithiothreitol
- CH_3COOH (to adjust the pH)

TG Hydrolase Assay Substrate

- 150 µl Triolein 100 mg/ml
- 75 µl PC/PI (3:1) 20 mg/ml
- 125 µCi radiolabelled Triolein (1 µCi/µl)

Potassium phosphate buffer

- 802 µl K_2HPO_4
- 198 µl KH_2PO_4
- Fill up to 20 ml with ddH_2O

RIPA (pH 7.5)

- 50 mM Tris/HCl
- 150 mM NaCl
- 0.5% Deoxycholate
- 1% NP-40
- 0.1% SDS
- 1:1000 Protease inhibitor
- Phosphatase inhibitor

4 mM Oleic acid complexed to BSA

- 24,3 mg oleic acid dissolved in 10 ml ddH_2O
- 3,4 mM fatty acid free BSA: 2 g in 10 ml 2 x PBS

Prewarm both solutions to 37°C and drop BSA solution to oleic acid solution while stirring.

DEPC water

- 1 l distilled water
- 1 ml DEPC
- autoclave

10x PBS (pH 7.3-7.4)

- 1.37 M NaCl
- 27 mM KCl
- 43 mM Na_2HPO_4
- 14 mM KH_2PO_4

Digestion buffer

- 0.03 g Collagenase D dissolved in 1 ml 1x PBS
- 600 µl 0.5 M HEPES
- 11 µl 2.5 M $CaCl_2$
- 500 µl BSA (20%)
- Fill up to 20 ml with 1x PBS

1x Protease inhibitors

- 20 µg/ml leupeptine
- 2 µg/ml antipain
- 1 µg/ml pepstatin

Maxiprep-DNA (NucleoBond Xtra Kit)

Elution Buffer

- Buffer salts
- 2-propanol 10-15%

Lysis Buffer

- Sodyium hydroxide solution 0.5-2.0%

Equilibration buffer

- Buffer salts
- Ethanol 5-20%

Neutralization buffer

Wash Buffer (pH 6.3)

- 100 mM Tris
- 15% EtOH
- 1.15 M KCl

AC binding buffer

- 50 mM TrisHCl
- 500 mM NaCl
- 5 mM Imidazol
- 10% Glycerol

Elution buffer

- 50 mM TrisHCl
- 500 mM NaCl
- 500 mM Imidazol
- 10% Glycerol

2.1.1 Protein determination

Pierce™ BCA Protein Assay (A:B 50:1) Thermo Scientific

- Pierce BCA Protein Assay Reagent A (#SI251119)
- Pierce BCA Protein Assay Reagent B -Prod (#1859078)
- 2 mg/ml BSA Standard Solution

Bradford Biorad

- Protein Assay Dye Reagent Concentrate (#500-0006)
- 2 mg/ml BSA Standard Solution

2.1.2 Kits

Infinity™ Triglyceride- Thermo Scientific

- Infinity Triglyceride (#236170)
- Glycerol Standard [2.5 mg/ml] – Sigma (#SLBN1724V)

NEFA -FUJIFILM

- NEFA-HR (2) R1a (21F18)
- NEFA-HR (2) R2a (22F18)
- NEFA Standard [1 mM] (12M18)

Glycogen- Megazyme

D-Glucose HK (L) KIT (#130511-1)

- Bottle 1: Buffer (pH 7.6)
- Bottle 2: coenzymes
- Bottle 3: HK/G6PDH
- Bottle 4: Standard [0.4 mg/ml in 0.2% benzoic acid]

Glycerol- Sigma

- Free Glycerol Reagent (#SLCB1540)
- Glycerol Standard [2.5 mg/ml] – Sigma (#SLBN1724V)

2.1.3 Agarose gel electrophoresis

1x TAE buffer (pH 7.2)

- 40 mM Tris-HCl
- 50 mM EDTA
- 7% acetic acid

Agarosegel 1.5%

- 4 ml 50 x TAE
- 3 g Agarose
- 196 ml ddH_2O

6x DNA Loading Dye

- 3 ml Glycerine
- 7 ml ddH_2O
- 25 mg Bromophenol blue
- 25 mg Xylencyonal

2.1.4 Quantitative polymerase chain reaction (qPCR)

Previous Kit

Perfecta DNAse I Kit- Quantabio (025858)

- 25 mM EDTA
- 2 U/µl Perfecta DNAse
- 10x DNAse I Reaction buffer

High capacity cDNA reverse transcription (Kit)- applied biosynthesis by Thermo Fisher (00767944)

- 50 Units/µl Multi scribe reverse transcriptase
- 4 U/µl Quiagen RNAse inhibitor
- 10 RT random primers
- 100 mM dNTP mix
- 10x RT Buffer

New Kit

DNAse I (RNAse free) New England Biolabs (NEB) #M0303L

- 50 mM EDTA
- 2,000 U/ml DNAse I
- 10x DNAse I Reaction Buffer

LunaScript RT SuperMix Kit, NEB #E3010G

- RT Supermix
- No-RT Control mix
- (5x concentration)

2.1.5 Western Blot (WB) analysis

4x Lower Buffer (pH 8.8)

- 1.5 M Tris-HCl

4x Upper Buffer (pH 6.8)

- 0.5 M Tris-HCl

CAPS-Transfer buffer (pH 11)

- 10 mM CAPS
- 10% Methanol

10x Tris- Glycine Buffer

- 200 mM Tris
- 1.6 M Glycin
- 0.83% SDS

Stripping Buffer (pH 6.7)

- 62.5 mM Tris-HCl
- 2% SDS

On the membrane: 20ml Stripping Buffer + 140 µl β-Mercaptoethanol

Coomassie staining solution

- 50% ethanol
- 7.5% from 80% acetic acid
- 0.25% Coomassie-brilliant blue R250

Coomassie destaining solution

- 10% from 80% acetic acid
- 30% methanol

Blocking solution

10% milk powder in 1x TST Buffer

1st Antibody

5% milk powder/BSA in 1x TST Buffer + AB in different dilutions

2nd Antibody

2% milk powder in 1x TST buffer + 1:10,000 AB

10x TST (pH 7.4)

- 1.5 M NaCl
- 500 mM Tris-HCl
- 1% Tween20

4x SDS loading dye (pH 6.8)

- 200 mM Tris-HCl
- 400 mM Dithiothreitol
- 8% SDS
- 40% Glycerine
- 0.05 % Bromophenol blue

2.1.6 Oil Red O' staining (ORO) & Thin layer chromatography (TLC)

Fixing solution (4% formaline)

- Dilute 37% formaldehyde in 1x PBS

ORO stock solution

- 500 mg Oil red O powder
- 100 ml 2-propanol abs.

ORO working solution

- ORO stock:dH_2O =3:2
- Incubation at 10 min at RT
- Through filter 0.45 µm

Thin layer chromatography reagent

- 10% copper sulphate
- 10% phosphoric acid
- Fill up to 200 ml ddH_2O

Eluent for TLC

- 70 ml Hexane
- 29 ml Diethylether
- 1 ml acetic acid

2.1.7 Media in cell culture

Table 2.1:Media and its ingredients

Media	**Ingredients**	**LOT number**	**Company**
Expi293 Expression medium	GlutaMAX-I	2043467	Gibco by life technologies
MEM α Medium (1X) Minimum essential medium	Ribonucleosides, Deox-yribonucleosides	1786983	
DMEM (1X) Dulbecco's modified eagle medi-um	1 g/L D-Glucose, L-Glutamine, Pyruvate	2062165	
	4.5 g/L D-Glucose, L-Glutamine, Pyruvate	2062233	
0.05% Trypsin- EDTA (1X)	Dissociation reagent	2063396	

ExpiFectamine 293 Transfection Kit- Gibco (2064536)

- OptiMEM
- Expifectamine
- Expi293 Enhancer 1
- Transfection Enhancer 2

Metafectene Transfection - Biontex (SEM202/RK101617)

2.1.7.1 Media Components

Freeze medium Expi cells

- 10% DMSO
- 45% new medium

Freeze medium OP9K cells

- 50% Fetal calf serum (FCS)
- 5% DMSO

Cos7 cells

Split medium

- DMEM (4.5 g/l glucose, L-glutamine, phenol red)
- 10% FCS
- 1% Penicillin-Streptomycin (PS)

3T3-L1 cells

Split medium

- DMEM (4.5 g/l glucose, L-glutamine, phenol red)
- 10% FCS
- 1% PS

Differentiation medium (d=0)

- Split medium
- 0.4 µg/ml Dexamethasone
- 10 µg/ml Insulin
- 500 µM 3-Isobutyl-1-methylxanthin (IBMX)

OP9K cells

Split medium

- Mem α Medium (1X)
- 20% FCS
- 1% PS

Selection medium (OP9K)

Selection concentration

- Split medium
- 2 µg/ml Puromycin
- 600 µg/ml Geneticin

Working concentration

- Split medium
- 0.2 µg/ml Puromycin
- 60 µg/ml Geneticin

Differentiation medium (OP9K)

- Memα (no adds)
- 10% FCS
- 1% PS
- 1 µg/ml Insulin
- 1:10 BSA-oleic acid complex

SVF of iWAT (primary adipocytes)

Split medium

- DMEM/F12 (1:1) (1x)
- Glutamax
- 10% FCS
- 1% PS

Differentiation medium (d=0)

- Split medium
- 1 µM Dexamethasone
- 0.87 µM Insulin
- 500 µM IBMX

LB medium (pH 7.0)

- 3 g NaCl
- 1.5 g Yeast extract
- 3 g peptone

adjust pH with 5 M NaOH

- After autoclaving, addition of ampicillin (100 µg/ml)

2.2 Chemicals

Standard chemicals were purchased from Merck (Darmstadt- Germany) or Roth (Karlsruhe-Germany) until otherwise stated.

- Albumin Fraction V, >98% powdered;
- Acetone, >99.8% pro analysi (p.a.)
- Bovine serum albumin (BSA) (FA free), >96% #SLBZ3578; pH7;
- Chloroform p.a. (CHEM-LAB, Bensheim-Germany)
- Ethanol, abs. 100% p.a. (CHEM-LAB, Bensheim-Germany)
- Ethidium bromide in TAE Buffer
- HCl smoking 37%, 36.46 M; density 1.19
- Hexane-(n) p.a., (CHEM-LAB, Bensheim-Germany)
- ITaq universal SYBR Green supermix (Biorad, Hercules-California-USA)
- Methanol, HPLC gradient grade (CHEM-LAB, Bensheim-Germany)
- Rotiszint eco plus; LSC-Universalcocktail, density 0.96
- SDS/NaOH (0.2%/0.3N)
- TRIzol Reagent -Ambion ^{R};(Life technologies, Carlsbad-California-USA)
- 1-Brom-3-Chloropropan; 157.44 M (PanReac-AppliChem GmBH, Darmstadt-Germany)
- 2-Propanol, >99.8% p.a.

2.3 WB analysis

2.3.1 SDS gel components

Table 2.2: SDS gel components

Separating gel	10% acrylamide	16.4 ml ddH_2O, 10 ml 4x lower buffer, 13.2 ml 30% acrylamide, 400 µl 10% SDS, 36 µl temed, 108 µl 10% APS
Stacking gel	4.5% acrylamide solution	4.13 ml ddH_2O, 1.75 ml 4x upper buffer, 1.05 ml 30% acrylamide, 70 µl 10 % SDS, 13.65 µl temed, 42 µl 10% APS, 0,5% blue dye
Standard	Colour Protein Standard broad range (BioLabs) #P7712S	
Plug solution	1x SDS sample buffer	

2.3.2 Antibodies used in WB analysis

Table 2.3: First antibodies and corresponding kDa

First antibodies	**kDa**
ATGL antibody #2138, cell signalling, 1:1,000 in 5% milk, rabbit, 2 h RT	54
PEDF antibody #ab14993, abcam, 1:1,000 in 5% BSA, rabbit, 4°C O.N.	50
PEDF antibody #MAB1059, chemicon, 1:1,000 in 5% BSA, mouse, 4°C O.N.	50

GAPDH antibody #2118 cell signalling, 1:30,000 in 5% BSA, rabbit, 1 h RT	37
His antibody #18184 abcam, 1:3,000 in 5% milk, mouse, 1 h RT	2 kDa + kDa of tagged protein

Antibodies were detected with chemiluminescence using ECL detection reagent and a Bio Rad Chemidoc System. Peroxidase-labelled secondary antibodies were used.

Table 2.4: Secondary antibodies

Secondary antibodies
Anti-rabbit antibody HRP 1:10.000 in 2% milk, 1 h RT; Vector Laboratories Inc. #ZE1026
Anti-mouse antibody HRP 1:10.000 in 2% milk, 1 h RT; GE Healthcare UK Ltd #14251045

2.4 Sequences of q-RT-PCR primer

Table 2.5: Primer pair sequences

Primer pair	**Sequence**	
36b4	36b4_fw	5'-GCT TCA TTG TGG GAG CAG ACA -3'
	36b4_rev	5'-CAT GGT GTT CTT GCC CAT CAG -3'
ATGL	ATGL_fw	5'- GAG ACC AAG TGG AAC ATC -3'
	ATGL_rev	5'- GTA GAT GTG AGT GGC GTT -3'
PEDF	PEDF_fw	5`-TCGGCTACGATCTGTACC-3´
	PEDF_rev	5`-AGCCCGGTGAATGACA-3´
mPref1	mPref1_fw	5'- AGAAAGGCCAGTACGAATGCTCCT -3'
	mPref1_rev	5'- TTGCGGCTACGATCTCACAGAAGT -3'
mPPARγ	mPPARγ_fw	5'- AACAAG ACTACC CTTTAC TGAAAT TACCA-3'
	mPPARγ_rev	5'- CAC AGA GCT GAT TCC GAA GTT G -3'
mAdipoQ	mAdipoQ_fw	5´-CCGGGACTCTACTACTTCTCTT 3´
	mAdipoQ_rev	5´-TTCCTGATACTGGTCGTAGGT-3´
C/EBPα	C/EBPα_fw	5' CAAGAACAGCAACGAGTACCG 3'
	C/EBPα_rev	5' GTCACTGGTCAACTCCAGCAC 3'

2.5 Reagents used in lipolysis experiments

The following reagents were used in lipolysis experiments. Triacsin C (TC) is an inhibitor of long FA acyl-CoA synthetase and de novo synthesis of TG, DG and CE (Dechandt et al. 2017). HSL inhibitor (Hi) inhibits the enzyme HSL, which hydrolyses DG as well as TG (Haemmerle et al. 2002), whereas Atglistatin (Ai) specifically inhibits ATGL (Mayer et al. 2014). Isoproterenol (iso) is a β-adrenergic agonist (https://pubchem.ncbi.nlm.nih.gov/compound/Isoproterenol; Accessed August 01. 2019).

2.6 Cell lines

2.6.1 Expi293

The Expi293™ Expression System constitutes a good transient expression technology. It allows rapid production (duration= 7 days) and high protein yield. (https://www.thermofisher.com; Accessed July 25.2019)

2.6.2 3T3-L1

These cells are preadipocytes developed by clonal expansion from murine swiss 3T3 cells. Preadipocytes can be differentiated to adipocytes using pro-differentiative agents. (https://www.ncbi.nlm.nih.gov/pmc/articles/PMC4573194/; Accessed July 17.2019)

2.6.3 OP9K

OP9 cells are derived from mouse bone marrow stromal cells. OP9K is a clonal population that differentiates fast and displays classic adipocyte morphology. (https://paperity.org/p/60310246/development-of-an-op9-derived-cell-line-as-a-robust-model-to-rapidly-study-adipocyte, Accessed July 17.2019)

2.6.4 Stromal-vascular fraction (SVF) of WAT

Adipose SVF consist of fibroblasts, macrophages, endothelial cells, preadipocytes and adult stem cells. (https://www.ncbi.nlm.nih.gov/pmc/articles/PMC5360317/; Accessed July 17.2019). Fractions were isolated and cultivated to differentiate them to primary adipocytes.

2.6.5 Cos7

This cell line was derived from the African green monkey and is kidney-fibroblast like. It was derived from the CV-1 cell line by transformation with an origin defective mutant of SV40 and therefore it is named Cos7 (www.thermofisher.com, Accessed July 17.2019).

2.7 Mouse model

For organ cultures and in vivo experiments, black6 mice (C57BL/6J) were used as mouse model. Usually, for experiments Wild type (WT) and PEDF-KO (PKO) mice on Chow diet were used but some experiments were performed using mice on high fat diet (HFD).“Chow diet” is the standard diet consisting of 12% fat, 26% protein and 62% carbohydrates, whereas HFD consists of 45% fat, 20% protein and 35% carbohydrates (SSNIFF Diets, http://www.ssniff.com/index.php, Accessed September 15.2019).

Most experiments were performed using male mice. Mice were housed at a typical 14 h light and 10 h dark cycle in thermostatic rooms (21-23°C). Usually, the mice had ad libitum access to water and food, unless otherwise stated. In all experiments, mice were aged between 10 - 18 weeks or 8 - 12 months.

2.8 Equipment

- Amersham Biosciences, Äkta prime plus, United Kingdom
- Azur Biosystems, absorbance microplate reader, USA
- Bartelt, Systec VX-150 Autoclave, Graz-Austria
- BANDELIN; Sonopuls & BANDELIN electronic UW 3100, Berlin-Germany
- BECKMAN; DU 640 Spectrometer, California- USA
- BECKMAN; GS-6 Centrifuge, California- USA
- BioRad; ChemiDoc Touch; Imaging System; Hercules-California-USA
- BioRad; Real-Time PCR Detection System; Hercules-California-USA
- BioRad; C1000TM Thermal Cycler; Hercules-California-USA
- Camag automatic TLC sampler 4, Muttenz, Switzerland
- Eppendorf; Centrifuge 5415 R, Hamburg-Germany
- Eppendorf; Thermomixer compact, Hamburg-Germany
- IKAR T10 basic- Homogenizer Workcenter; Ultraturrax; Staufen-Germany
- Julabo waterbath (MP), Seelbach-Germany
- Labconco, CentriVap Concentrator (Speed vac), Kansas City-USA
- Merck, Analytical Chromatography, TLC Silica gel 60, Darmstadt-Germany
- Packard, 1900CA- TRI-CARB liquid scintillation analyzer (Counter), Palo Alto-California
- PeQlab Biotechnologie GmbH; Nanodrop ND-100; Spectrophotometer; Berlin-Germany
- Pharmacia Biotech Inc.; Electrophoresis Power Supply- EPS600, Northamerica-USA
- Thermo Fisher Scientific; Multiskan FC; Massachusetts- USA
- Thermo Fisher Scientific, StepOnePlus Real-Time PCR System, Massachusetts- USA
- WellionR Calla classic, MED TRUST GmbH, Glucometer, Marz-Austria

3. Methods

3.1 Transformation of chemical competent cells & Maxiprep

Chemical competent cells were thawed 5 min on ice. Plasmids had to be diluted with Fresenius water 1:10 to a final concentration of 100 ng/µl. 25 µl cells were mixed with 1 µl plasmid and as a negative control with 1 µl Fresenius water. After an incubation for 30 min on ice, cells were heat shocked for 30 sec at 42°C in a water bath. Then samples were cooled on ice water and 250 µl SOC medium (prewarmed at 37°C) were added. After an incubation for 1 h at 37°C under shaking, 50 µl cell solution was plated on a 37°C prewarmed LB + ampicillin (amp) plate (see 2.1.7) and incubated at 37°C until the next day. For each selected bacterial colony an overnight culture (LB + amp) of 5 ml was prepared. Glycerol stocks were prepared by mixing 500 µl overnight culture [pEDF-Cterm His-FLAG CMV5.1] with 500 µl glycerol.

For high yield plasmid purification (Maxiprep) 5 ml culture were incubated for 8 h at 37°C. 1 ml of the preculture was used to inoculate 250 ml medium. For Maxiprep, cells were centrifuged at 5,000 g for 10 min at 4°C. The pellet was resuspended in 12 ml RES buffer, followed by the addition of 12 ml lysis Buffer (see 2.1). While incubating the cells for 5 min, the column was equilibrated with 25 ml EQU buffer (see 2.1). Then, 12 ml of neutralization buffer (see 2.1) were added to the cell suspension and the whole suspension was transferred to the column. The column was washed once with 15 ml EQU buffer and once with 25 ml wash buffer (see 2.1). To the plasmid DNA, 15 ml elution buffer (see 2.1) were added and liquid was collected. Precipitation was performed using 10.5 ml 100% isopropanol. After the sample was vortexed and centrifuged at 15,000 g for 30 min at 4°C, the pellet was washed with 4 ml 70% ethanol and centrifuged for 10 min at RT. The supernatant was removed and the pellet dried for ~25 min at 37°C. Then, the DNA Pellet was dissolved in 200 µl Fresenius water and transferred to a new tube. Another 200 µl were used to rinse the previous tube. In total, 400 µl of plasmid DNA were obtained and concentration was determined using Nanodrop (see 2.8). To obtain a concentration of 1 µg/µl plasmid DNA, a volume of 640 µl Fresenius water was added. The maxiprep stock was frozen at -20°C until further use.

3.2 Cell culture

3.2.1 Freeze and thaw procedure

Freeze cells

Cells were harvested at 290 g for 3 min at RT. The pellet was resuspended in 1 ml medium and filled up with medium to 3 ml. In each cryo vial, 1 ml cell suspension and 1 ml freeze medium (see 2.1.7.1) were added and slowly frozen using an isopropanol container.

Thaw cells

To thaw cells, 1 ml prewarmed medium was added to the frozen cells and transferred to a tube containing 14 ml medium. They were centrifuged at 290 g for 3 min at RT and the pellet was dissolved in fresh medium. Then, the cells were transferred to a 75 m^2 flask and incubated at 37°C.

3.2.2 Cell splitting

To split cells, medium was removed, and cells were washed with 10 ml 1x PBS. Furthermore, 3 ml trypsin were added and incubated for 3 min at 37°C to detach the cells from the flask bottom. The reaction was stopped by adding 10 ml medium containing 10% FCS. The suspension was transferred to a new tube and centrifuged at 290 g for 3 min at RT. The pellet was resuspended, and the cells were split 1:2 up to 1:8 depending on the cell type.

3.3 DNA purification

3.3.1 Transfection of Expi cells using Expifectamine

Expi cells were cultured in 25 ml Expi293 expression medium in shaking bottles. They have a doubling time of 1 day. The day before transfection, cells were seeded at a density of $2.5*10^6$ cells/ml. 30 µg plasmid DNA PEDF-His (C-terminal) were mixed with 1.5 ml OptiMeM medium (see 2.1.7) and 80 µl Expifectamine (see 2.1.7) were mixed with 1.5 ml OptiMeM medium. Both solutions were incubated for 5 min at RT. Then solutions were mixed and incubated for 20 min at RT. The DNA-reagent complex was added to the cells (without FCS) and incubated for 16-18 h. The next day, transfection enhancer 1 (150 µl) and enhancer 2 (1.5 ml) were added to the cells and incubated for 2-4 days.

3.3.2 Purification of His tagged proteins using Äkta

Cells were harvested at 290 g, 3 min at RT and the medium was filtered through a 45 µm filter. The medium was used for the purification process and filled up to 40 ml with AC binding buffer (see 2.1). At first, the system had to be washed by putting the tube of position A=1 and position 2 into the AC binding buffer and the tube of position B (middle), into the elution buffer (see 2.1). The following program was chosen: 'Program_Template_Application template_system wash' with a pressure of 10-50 ml/min flow rate and on column 1 ml/min flow. Afterwards, the tube at position 2 had to be washed manually with 30 ml AC binding buffer and the column was loaded with the sample (35 ml medium). The tube was put into 40 ml binding buffer to make sure all the protein was loaded on the column. After approx. 1 h protein gradient elution started, and fractions were collected. Afterwards, the system had to be washed with water.

Fractions which contained the protein of interest were pooled, dialysed in AC binding buffer overnight and protein concentration was determined using Bradford. PEDF-His protein had a concentration of 1) 0.27 µg/µl and 2) 0.769 µg/µl and was stored at -20°C. To determine whether the protein was well purified, it was analysed on a 10% SDS gel.

3.3.3 Transfection of Cos7 cells

The evening before transfection, cells were seeded at a density of 900,000 cells/10 cm dish, which is an amount of 15,500 cells/cm². The next day, medium was changed to 3 ml DMEM without PS. Then two tubes were prepared for each condition (LacZ and PEDF) containing:

1) 6 µg DNA + 300 µl DMEM (-/-)
2) 27 µl Metafectene (see 2.1.7) + 300 µl DMEM (-/-)

Both solutions were mixed and incubated for 20 min at RT. Afterwards, this complex was added directly to the medium of the cells and incubated for 4 h at 37°C. Thereafter, the medium was removed and 8 ml DMEM (PS+10% FCS) were added. The next day, the medium was changed to 8 ml DMEM with PS and only 1% FCS, which was then used as conditioned medium for lipolysis experiments.

3.3.4 3T3-L1 cells

These cells should not get too dense as they do not differentiate well anymore.

To differentiate 3T3-L1 cells, they were seeded in 6, 12 or 24 well plates and cultivated until confluency (~2 days). Two days post-confluent, medium was changed (d=0) and differentiation started.

Day 0

Table 3.1: Differentiation medium components of 3T3-L1 at day 0

	Initial concentration	**Solvent**	**Final concentration**
Split medium (see 2.1.7.1) +			
Dexamethason	0.5 mg/ml	EtOH	0.4 µg/ml
Insulin	10 mg/ml	H_2O	10 µg/ml
IBMX	500 mM	DMSO	500 µM

- IBMX had to be preheated at 60°C for 5 min prior to use.

Day 3

Table 3.2: Differentiation medium components of 3T3-L1 at day 3

	Initial concentration	**Solvent**	**Final concentration**
Split medium +			
Insulin	10 mg/ml	H_2O	10 µg/ml

Day 5 + 7

Table 3.3: Differentiation medium components of 3T3-L1 at day 5+7

	Initial concentration	**Solvent**	**Final concentration**
Split medium +			
Insulin	10 mg/ml	H_2O	0.2 µg/ml

At day 8 experiments were performed.

3.3.5 OP9K cells

To differentiate OP9K cells, they were seeded in 6, 12 or 24 well plates and cultivated until confluency (~2-3 days). Two days post-confluent medium was changed, and differentiation started. Every second day, differentiation medium (see 2.1.7.1) was changed and after 3-4 days, experiments were performed.

3.3.6 Stromal-vascular fraction (SVF) of white adipose tissue

At first, iWAT (inguinal white adipose tissue) was dissected, put into 1x PBS on ice, and cut into small pieces. Tissue pieces were digested using 10 ml digestion buffer (see 2.1). After 45 min incubation at 37°C under shaking (110 rpm), reaction was stopped by adding 20 ml medium (see 2.1.7.1). Then, mechanically digestion with a stripette was performed and the suspension filtered through a 100 µm filter. Afterwards, the sample was centrifuged at 382 g for 5 min. The pellet contained cells, which were resuspended in 1 ml medium, filled up to 5 ml, and filtered through a 40 µm filter. Another 5 ml of medium were used to rinse the filter. The centrifugation step was done twice followed by seeding of 1 ml of the cells in 10 cm dishes containing a volume of 9 ml. Cells were incubated at 37°C. Afterwards, they were transferred to a 175 cm² flask and further seeded into 12 well or 24 well plates. These cells were differentiated 3 days post confluency.

<u>Day 0 & 1</u>

Table 3.4: Differentiation medium components of primary adipocytes at day 0+1

	Solvent	**Final concentration**
Split medium (see 2.1.7.1)		
Dexamethason	EtOH	1 µM
Insulin	H_2O	0.87 µM (=5 µg/ml)
IBMX	DMSO	0.5 mM

Day 2+4+6

Table 3.5: Differentiation medium components of primary adipocytes at day 2+4+6

	Solvent	Final concentration
Split medium		
Insulin	H_2O	0.87 µM

3.4 Lipolysis Experiment

After cells were completely differentiated (f.e. in a 24 well plate), lipolysis experiment was performed. Therefore, medium was removed and 300 µl medium containing components such as rPEDF, TC or iso were added to the cells for 30 min preincubation. Afterwards, medium was removed and 300 µl of new medium containing same components plus 2-3% BSA were added. The cells were incubated 2 h for basal and 1 h for iso stimulated lipolysis at 37°C. This medium was collected in a 96 well plate and FA as well as glycerol content was determined (see 3.10).

To determine the protein concentration, cells were washed three times with 1x PBS, followed by the addition of 500 µl hexane isopropanol (3:2), which extracts lipids. After 5-10 min incubation time at RT, it was removed, and protein was lysed in 500 µl SDS/NaOH (0.2%/ 0.3N) for ~3 h at RT. Protein concentration was determined using BCA method (see 3.5B).

3.5 Protein determination

A) **Bradford (Biorad)**

Bradford reagent was prepared 1:5 in ddH_2O. BSA (2 mg/ml) diluted in ddH_2O was prepared as standard with a dilution series from 1:5 to 1:160. Samples were diluted in ddH_2O. In each well (96 well plate) 20 µl of sample and 150 µl of reagent were added. After short incubation at RT, extinction was detected at 560 nm by using Multiscan FC (see 2.8). Protein concentration was calculated using a standard curve.

B) **Bicinchoninic acid assay (BCA) (Thermo Scientific)**

BSA (2 mg/ml) diluted in SDS/NaOH (0.2%/0.3 N) was prepared as standard, starting with a 1:2 dilution up to a 1:64 dilution. Samples were diluted in SDS/NaOH (0.2%/0.3N).

In a 96 well plate (Greiner; Bioone; Kremsmünster) 10 µl sample and 150 µl BCA reagent (see 2.1.1) were added and incubated at 37 °C for 30 min. Extinction was detected at 560 nm via Multiscan FC (see 2.8). Protein concentration was calculated using a standard curve.

3.6 Oil red O' (ORO) staining of adherent cells

Cells were washed twice with 1x PBS. Then, cells were fixed by adding 500 µl fixing solution (see 2.1.6) and incubated for 15 min at RT. Afterwards, cells were washed twice with dH_2O as well as with 60% isopropanol. After cells were dried, they were incubated with 500 µl ORO working solution (see 2.1.6) for 45 min at RT. Cells were again washed with dH_2O and the dye extracted by adding 500 µl isopropanol and shaking for 15 min at RT. The dye in the isopropanol fraction was measured using the plate reader (see 2.8) at 492 nm. The amount of lipids was related to protein concentration.

3.7 Triglyceride determination

3.7.1 Preparation of cells

At different times (d=0, 1, 2, 3) of differentiation, cells were analysed for their TG content. Therefore, cells were washed three times with 1x PBS, followed by addition of 3x 600 µl hexane isopropanol (3:2). After 10 min at RT, solvent was collected each time and evaporated under vacuum in speed vac (see 2.8) at 37°C, until lipids were dried. Then, the tube was washed with 300 µl of chloroform and evaporated. Dried lipids were resolved in 200 µl 2% Triton X100 in H_2O by sonication 2 x 5 sec (amplitude 10%). Acyl glycerol content was measured using infinity kit and glycerol as standard (dissolved in 2% Triton X100 in H_2O). Protein concentration of the cells was measured using the BCA method and BSA as standard. TG concentration was calculated using a glycerol standard curve, which was related to the protein concentration.

3.7.2 Preparation of tissue

To isolate neutral lipids, ~15 mg of liver powder was extracted using the method of Folch. After vortexing four times within 30 min, the samples were incubated in a thermoblock (see 2.8) at 21°C and 900 rpm for 30 min. Then the samples were centrifuged at 1,137 g for 10 min at RT and the organic phase was collected using a hot needle or a pipette. Then,

500 µl of the organic phase were evaporated under nitrogen at 37°C and resolved in 300 µl 2% Triton X100 in H_2O by sonication 2 x 5 sec (10% amplitude). Acyl glycerol content of the organic phase was measured using infinity kit and glycerol as standard (dissolved in 2% Triton X100 in H_2O). Protein concentration of the pellet was measured using the BCA method and BSA as standard. TG concentration was calculated using a glycerol standard curve and related to the protein concentration.

3.8 TG-Hydrolase Activity Assay

First, tissue had to be disrupted in 500 µl solution A (see 2.1) using Ultra Turrax Homogenizer (see 2.8). Tissue homogenates were centrifuged at 16,000 g for 30 min at 4°C, infranatant collected and protein concentration determined using Bradford reagent. For TG-hydrolase activity assay, 20 µg of protein were used. Samples were prepared in a total volume of 100 µl solution A (see 2.1) in assay tubes.

- 1x sample
- 1x sample + Ai
- 1x sample + Hi.

Substrate (1.67 mM) was prepared in two tubes, each containing 150 µl Triolein (100 mg/ml), 75 µl PC:PI (20 mg/ml) and 250 µl radioactive labelled Triolein (3H). Substrate was evaporated under nitrogen to get rid of all solvent. 1 ml of 100 mM potassium phosphate buffer (see 2.1) was added and sonicated (see 2.8) for 30 sec on ice (12% amplitude) and rested for 30 sec. This was repeated three times. Then the substrate was filled up with potassium phosphate buffer to a volume of 9 ml. Both substrates were mixed and 2 ml of 20% FA free BSA were added. 100 µl substrate was incubated with the sample for 1 h at 37°C in a water bath under shaking. The reaction was stopped by adding 3.25 ml of methanol, chloroform and n-heptane solution (10/9/7) as well as 1 ml of 0.1 M potassium carbonate. Each sample was vortexed for 6 sec and frozen until the next day.

The next day, samples were thawed for minimum 30 min at RT and vortexed. Then, they were centrifuged at 650 g for 10 min. 8 ml of scinti cocktail were added into scintillation vials and 500 µl supernatant of the samples was transferred to it. For determination of specific substrate activity, 20 µl of the substrate were measured. Radioactivity of the samples was determined using a β-counter (see 2.8).

For the calculation, 1.67 mM substrate was used.

$$Substrate\ conc. = \frac{\frac{1.67}{1000}(\mu mol)}{10\ (pro\ 100\ \mu l)} = 0.167\ \frac{\mu molTO}{Assay} = 0.501\ \mu mol\ FA/Assay$$

$$501\ nmol\ FA = counts\ per\ minute\ (cpm)\ of\ substrate$$
$$1\ nmol\ FA = x\ cpm$$

$$nmol\ FA\ of\ sample = \frac{(Cpm\ sample - Blank)}{x\ cpm\ (1\ nmol\ FA)}$$

$$nmol\ FA/mg\ protein = \frac{nmol\ FA\ of\ sample}{20\ \mu g\ protein} * 1000$$

A correction of the calculation was performed. The upper phase consisted of 2.45 ml but only 500 µl were counted. Also, only 71.5% of total FA were extracted to the upper phase. Therefore, these corrections had to be included into the calculation.

3.9 Glycogen determination

Liver powder (~30 mg) was homogenized in 1 ml 0.03 M HCl on ice using an Ultra Turrax (see 2.8). Free glucose content was obtained by adding the same volume 2 M HCl to an aliquot of liver homogenate and immediately neutralizing with 2 M NaOH, and using Hexokinase Kit.

Glycogen was hydrolysed by the addition of 2 M HCl at 90°C for 2 h. The solution was neutralized using 2 M NaOH. Glucose was measured using the Hexokinase Kit.

The Hexokinase Megazyme Kit (see 2.1.2) was downscaled to 400 µl H_2O, 20 µl sample, 20 µl of solution 1 and 20 µl of solution 2. After incubation for 3 min at RT, samples were measured at 340 nm followed by the addition of 3 µl solution 3. Thereafter, samples were incubated for 10 min at RT and detected at 340 nm. To obtain glycogen content, free glucose was subtracted from total glucose.

3.10 FA, glycerol and TG determination

FA determination

10-40 µl sample was incubated with 100 µl of R1A solution (see 2.1.2). After incubation for 10 min at 37°C, 50 µl of R2A solution were added and again incubated for 10 min at 37°C. As standard NEFA [1 mM] was used. Then, absorption was measured at 560 nm.

Glycerol determination

Glycerol content was determined by incubating 10-40 µl sample with 150 µl of glycerol reagent (see 2.1.2) for 10 min at 37°C. Extinction was determined at 560 nm. The standard curve was performed using glycerol [2.82 mM].

TG determination

TG content was determined using 150 µl of Infinity reagent (see 2.1.2). 10-40 µl sample were incubated for 10 min at 37°C and measured at 492 nm. The standard curve was performed using glycerol [2.82 mM].

3.11 Thin layer chromatography (TLC)

The organic phase obtained from chapter 3.7 was used for further analysis with TLC. Therefore, samples were diluted 1:4 with chloroform p.a. and transferred to a silica gel plate (see 2.8) using an automatic sampler (see 2.8). As standard, 100 µl mixture of TG, DG and MG were used. While the robot applied 20 µl of samples and 5 µl of standard, the TLC chamber was saturated with solvent (70 ml hexane, 29 ml diethylether, 1 ml acetic acid). After 45 min the robot had finished, and the silica gel plate was placed in a chamber containing mobile solvent (see 2.1.6). Afterwards, the plate was incubated with copper sulphate reagent (see 2.1.6) and dried at RT. Once the plate was dry, it was incubated at 120°C for 30 min to visualize bands.

3.12 RNA Isolation and RT-qPCR

3.12.1 Preparation of cells

For RNA isolation, 500 µl trizol (see 2.2) were added to the cells and collected. Then, 100 µl chloroform (see 2.2) were added, shaken for approx. 15 sec and incubated at RT for 3 min.

After centrifugation step at 12,000 g, 4°C for 15 min, 250 µl of isopropanol (see 2.2) were added and centrifuged again at 15,000 g for 40 min at 4°C. Pellet was washed twice with 500 µl 75% cold ethanol (see 2.2) and centrifuged for 10 min at 16,000 g and 4°C. The following procedure is the same as described in the next step.

3.12.2 Preparation of tissue

For RNA Isolation 1-3 shovel of tissue powder were homogenized in 1 ml trizol (see 2.2) on ice using an Ultra Turrax (see 2.8). After 5 min incubation at RT, 0.1 ml 1-bromo-3-chloropropane were added to the samples and incubated 10 min at RT followed by centrifugation at 12,000 g and 4°C for 15 min. The aqueous supernatant was transferred to a fresh tube. RNA precipitation was achieved by adding 0.5 ml isopropyl alcohol. After centrifugation for 10 min, 12,000 g at 4°C, the supernatant was removed. Afterwards, the pellet was washed twice using 1 ml 75% ethanol in Diethyl pyrocarbonate (DEPC) water (see 2.1) by centrifugation at 7,500 g for 5 min at 4°C. Then, the supernatant was removed and the pellet dried. RNA was dissolved in DEPC water and RNA concentration was measured via Nanodrop (see 2.8). The ratio of the absorbance at 260 and 280 nm (A260/280) was used to assess the purity of nucleic acids. The ratio for pure RNA A260/280 is ~2.0.

RNA was diluted 200 ng/µl RNA in a volume of 20 µl. To analyse integrity of the isolated RNA, 5 µl were separated by electrophoresis (1.5% agarose gel).

3.12.3 Previously used Kit

Another 5 µl RNA were used for DNAse I digest. Therefore, RNA was incubated with 1 µl DNase [1 U/µl], 1 µl 10x DNase-buffer and 3 µl DEPC-H_2O in PCR cycler for 30 min at 37°C. The reaction was stopped by adding 1 µl 25 mM EDTA and again incubated for 10 min at 65°C.

For reverse transcription, 10 µl of RNA were mixed with 2 µl 10x RT buffer, 0.8 µl dNTPs (100 mM), 2 µl 10x random primer, 1 µl reverse transcriptase, 0.1 µl RNAse inhibitor and 4.1 µl n. f. H_2O. Samples without reverse transcriptase were used as negative control. After carefully mixing, the samples were placed into a thermocycler (see 2.8) to transcribe RNA into complementary DNA (cDNA).

Table 3.6: previous used thermocycler program

Thermocycler program	**Step 1**	**Step 2**	**Step 3**	**Step 4**
Temperature [°C]	25	37	85	4
Time [min]	10	120	5	forever

Thereafter, cDNA was diluted 1:5 (freeze -20°C) and 1:25 for qPCR.

qPCR was performed in a 96 well plate (BioRad; Hercules-California-USA). Therefore 4 µl cDNA were incubated with 10 µl SYBR Green Mix (BioRad; Hercules-California-USA), 1 µl forward primer (fw, 10 pmol/µl), 1 µl reverse primer (rv, 10 pmol/µl) and 4 µl H_2O.

Table 3.7: previous used temperature protocol for Reverse Transcriptase qPCR

Temperature protocol for RT-qPCR			
Initial steps		Each of 40 cycles	
Hold (once)	Hold (once)	Melt	Anneal/Extend
2 min	10 min	15 sec	1 min
50°C	95°C	95°C	60°C

Using the program shown in table 12, a melt curve and amplification graph for analysing the cDNA in each sample was obtained.

3.12.4 New cDNA synthesis Kit (BioLabsInc., New England)

This was used for feeding-fasting experiments. 5 µl of RNA were used for DNAse I digest. Therefore, RNA was incubated with 0.5 µl DNase, 1 µl 10x DNase-buffer and 3.5 µl n. f. H_2O at 37°C for 10 min. The reaction was stopped by adding 1 µl 50 mM EDTA and again incubated for 10 min at 75°C.

For reverse transcription, 10 µl of RNA were mixed with 6 µl n. f. H_2O and 4 µl Luna Script RT Supermix containing RT buffer, dNTPs, random primer, reverse transcriptase and RNAse inhibitor. Samples without reverse transcriptase were used as negative control. After carefully mixing, the samples were placed into a thermocycler (see 2.8) to transcribe RNA into cDNA.

Table 3.8: New cDNA Synthesis thermocycler program

Thermocycler program	**Primer Annealing**	**cDNA Synthesis**	**Heat inactivation**
Temperature [°C]	25	55	95
Time [min]	2	10	1

Thereafter, cDNA was diluted 1:5 (frozen at -20°C) and 1:25 for qPCR.

qPCR was performed in a 96 well plate (Biozym). Therefore, 4 µl cDNA were incubated with 10 µl SYBR Green Mix (BioRad), 1 µl forward primer (fw, 10 pmol/µl), 1 µl reverse primer (rv, 10 pmol/µl) (table 13) and 4 µl n. f. H_2O.

New equipment was used (Applied Biosystems- StepOnePlus Real time PCR system).

Table 3.9: New temperature protocol for Reverse Transcriptase qPCR

Temperature protocol for RT-qPCR			
Initial steps		Each of 40 cycles	
Hold (once)	Hold (once)	Melt	Anneal/Extend
2 min	10 min	15 sec	1 min
50°C	95°C	95°C	60°C

3.13 WB analysis

3.13.1 Preparation of cells

12 well plates were put on ice. Then, 500 µl of Radioimmunoprecipitation assay buffer (RIPA) were added (see 2.1) and cells were incubated for 15 min. Afterwards, cell lysate was transferred from the plate to 1.5 ml tubes and sonicated 2x 5 sec with 13% amplitude. The lysate was centrifuged at 1,000 g for 15 min at 4°C and BCA protein determination was performed on the infranatant. Thereafter, acetone precipitation was performed. Therefore, five times more acetone than sample was added, and precipitation was carried out at -20°C overnight. The next day, samples were centrifuged at 16,000 g and 4°C for 30 min; and pellet was dissolved in 12 µl 1x SDS sample buffer.

3.13.2 Preparation of tissue

Approx. 30 mg tissue was homogenized using an Ultra Turrax (see 2.8) in 600 µl solution A (see 2.1) on ice and centrifuged at 1,000 g for 30 min at 4°C. Afterwards, the infranatant was transferred to a new tube and protein concentration was determined using Bradford reagent. Alternatively, 80 µl of the lysate were precipitated with 600 µl ice cold acetone overnight at -20°C. Protein precipitates were pelleted at 16,000 g, 4°C for 30 min. Then the pellet was dissolved in solution A + SDS sample buffer (see 2.1.5).

3.13.3 Procedure of WB analysis

30 µg protein (see 3.13.1,2) was subjected to sodium dodecyl sulphate-polyacrylamide gel electrophoresis (SDS-PAGE). Electrophoresis was performed using a 10% SDS-gel at 600 V and 40 mA for about 1 h to separate the proteins according to their molecular weight by using an electrophorese buffer (see 2.1.5). Proteins were blotted to a polyvinylidene difluoride (PVDF) membrane in CAPS buffer (see 2.1.5) at 600 V and 200 mA for 1:10 h. Afterwards, the membrane was incubated with 10% milk powder (in 1x TST) for at least 2 h to block unspecific binding sites. For detection of proteins different primary antibodies were used in different dilutions (see 2.3) and incubation time. Secondary, horseradish peroxidase labelled, antibodies were diluted 1:10,000 in 2% milk powder (1x TST) and visualized using ECL detection reagent and a Bio Rad Chemidoc System (see 2.8).

3.14 Cold exposure experiment

Wildtype (WT) and PEDF knockout (PKO) mice were put into cold at 5°C with no food for 6 h. After 0 h, 3 h and 6 h, temperature was measured and at time 6 h blood was collected to analyse plasma parameters as well as glucose content. One-week later blood was collected, which is time 0 h of cold exposure. Blood was centrifuged at 4°C, 2,300 g for 10 min. Supernatant was collected and used for further analysis like FA, glycerol and TG content measurements (see 3.10).

3.15 Fat pad assay

The left gWAT (gonadal white adipose tissue) of each mouse was excised, washed in 1x PBS and weighed. Each half of a depot was put in a cell strainer (100 µm), positioned in a 6 well plate containing 5 ml DMEM 1g/L glucose + PS (=preincubation). Using a small scissor, the

depot was cut into pieces of approx. 20 mg. Afterwards, fat pads were washed via transfer of the cell strainer into 1x PBS (10 cm dish) followed by drying on a piece of paper. Then they were placed into a new 6 well plate containing 5 ml DMEM 1g/L glucose + 2% FA free BSA (see 2.1.7, 2.2). After 2 h basal incubation time at 37°C and 5% CO2 under shaking, the cell strainers were washed as described before and then put into a new 6 well plate containing 5 ml DMEM 1g/L glucose + 1 µM iso. After 30 min preincubation time, the same ingredients were used plus 2% BSA for 1 h iso stimulated incubation. After each incubation medium was collected for further analysis like FA and glycerol measurement (see 3.10).

Afterwards, fat pieces were transferred to 4 ml Folch (CHCl3/MeOH 2:1) and 1 ml water in RNA tubes to remove fat for 2 h on the top over wheel. Tubes were centrifuged for 10 min at 2451 g and supernatant was decanted to let the pellet dry. Then, fat pads were incubated with SDS/NaOH (0.4%/0.2N) at 55°C on the shaker overnight to lyse them. Protein concentration was determined using BCA and BSA as standard (see 3.5B).

3.16 Statistics

All experimental results are shown as means and standard deviation. Statistical significance was determined using Student's t-test ($p \leq 0.05$ =*, 0.01=**, 0.001=***). Nalimov outlier test was performed to identify statistical outliers.

4. Results

4.1 Characterisation of PEDF deficient mice

Several previous reports suggested a role of PEDF in lipid metabolism. To get a better understanding how PEDF deficiency affects lipid metabolism, I first determined plasma parameters, tissue weights, and expression of PEDF and ATGL in tissues of fed and fasted WT and PEDF-KO (PKO) mice.

For this purpose, mice were fasted overnight or fasted overnight and refed for 2 h. After body weight determination and blood sampling, mice were sacrificed and tissues collected for further experiments (qPCR, Western blot (WB)). Thereafter, plasma parameters including FA, glycerol and TG content were analysed.

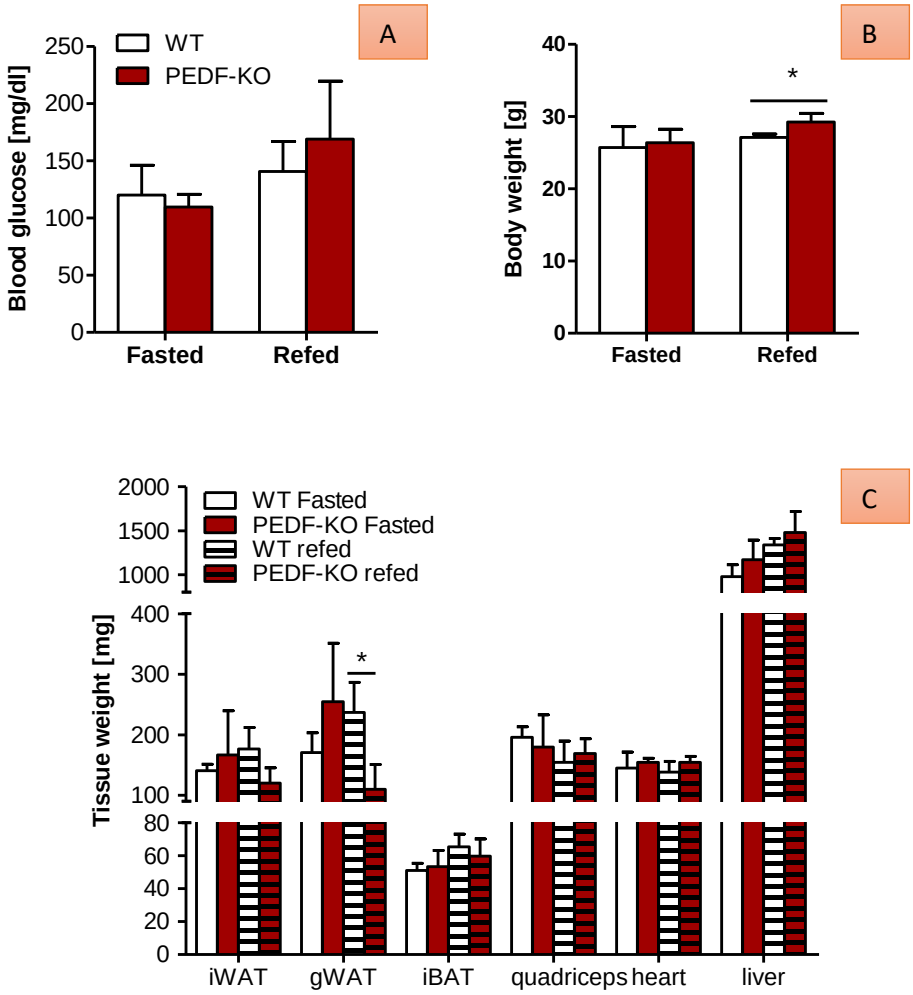

Figure 4.1: Blood glucose, body weight and tissue weight of WT and PKO male mice. 14-18 weeks old mice were fasted overnight or fasted overnight and refed for 2 h. Blood glucose (A) was measured using a glucometer. Body weight (B) of mice and tissue weight (C) was determined. Data are shown as mean + standard deviation (n=3). Significance was determined by Student's t-test ($p \leq 0.05$ =*, 0.01=**, 0.001=***).

As shown in figure 4.1.A, B, the blood glucose and body weight increased upon refeeding compared to fasting. While no difference in blood glucose and body weight is observed between WT and PKO mice in the fasted state, there is a trend towards increased glucose (1.2-fold), and significant increased body weight (1.1-fold) of PKO mice in the refed state.

In figure 4.1.C, weights of adipose -, muscle tissue and liver are shown. Upon fasting WT mice reduced the size of AT (-28% gonadal white adipose tissue (gWAT) and -20% inguinal white adipose tissue (iWAT)) resulting from increased lipid mobilization. However, PKO mice had increased fat depots (gWAT 2.3-fold, iWAT 1.4-fold) in the fasted state compared to the fed state. Moreover, refed gWAT was 54% reduced in PKO mice compared to WT mice.

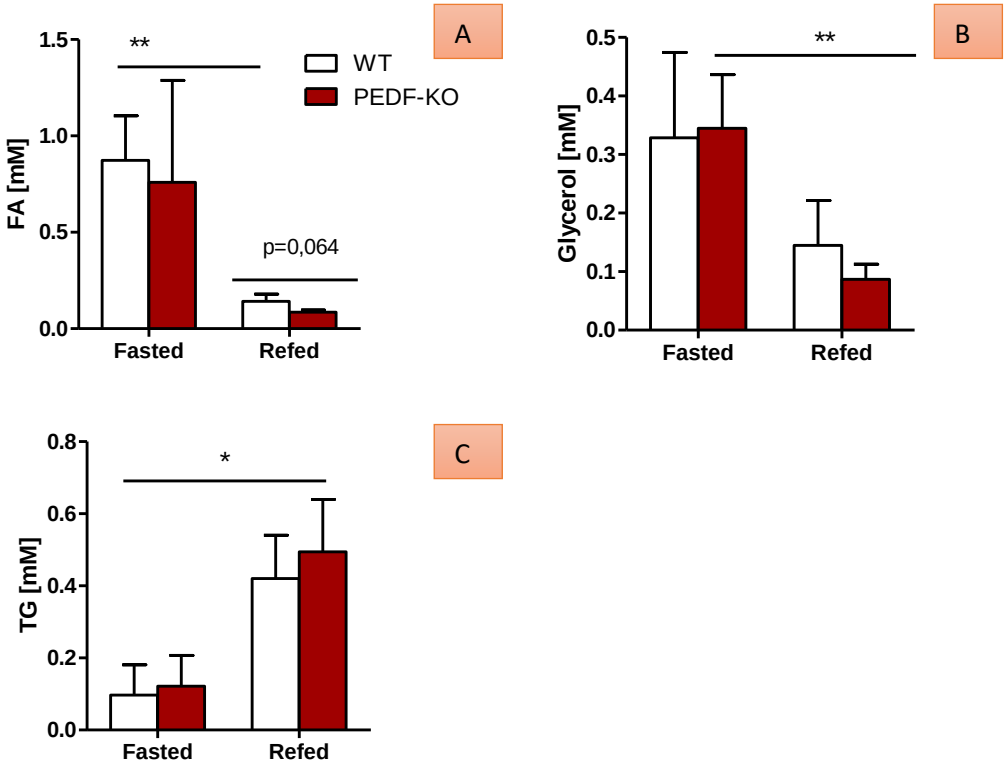

Figure 4.2: Plasma parameters of WT and PKO male mice. 14-18 weeks old mice were fasted over night or fasted overnight and refed for 2 h. FA (A), glycerol (B) and TG content (C) was determined in plasma using a comercial colorimetric kit. Data are shown as mean + standard deviation (n=3). Significance was determined by Student's t-test ($p \leq 0.05$ =*, 0.01=**, 0.001=***).

FA, glycerol and TG concentration in the plasma showed a clear feeding-fasting response. FA content was reduced by ~86%, and glycerol content was reduced by ~56% in the refed compared to fasted WT and PKO animals. TG concentration was increased by 4.3-fold in the refed compared to fasted WT and PKO mice.

To determine whether PEDF deficiency affects ATGL protein and mRNA expression, I did WB analysis and performed q-RT-PCR on tissue samples of WT and PKO mice.

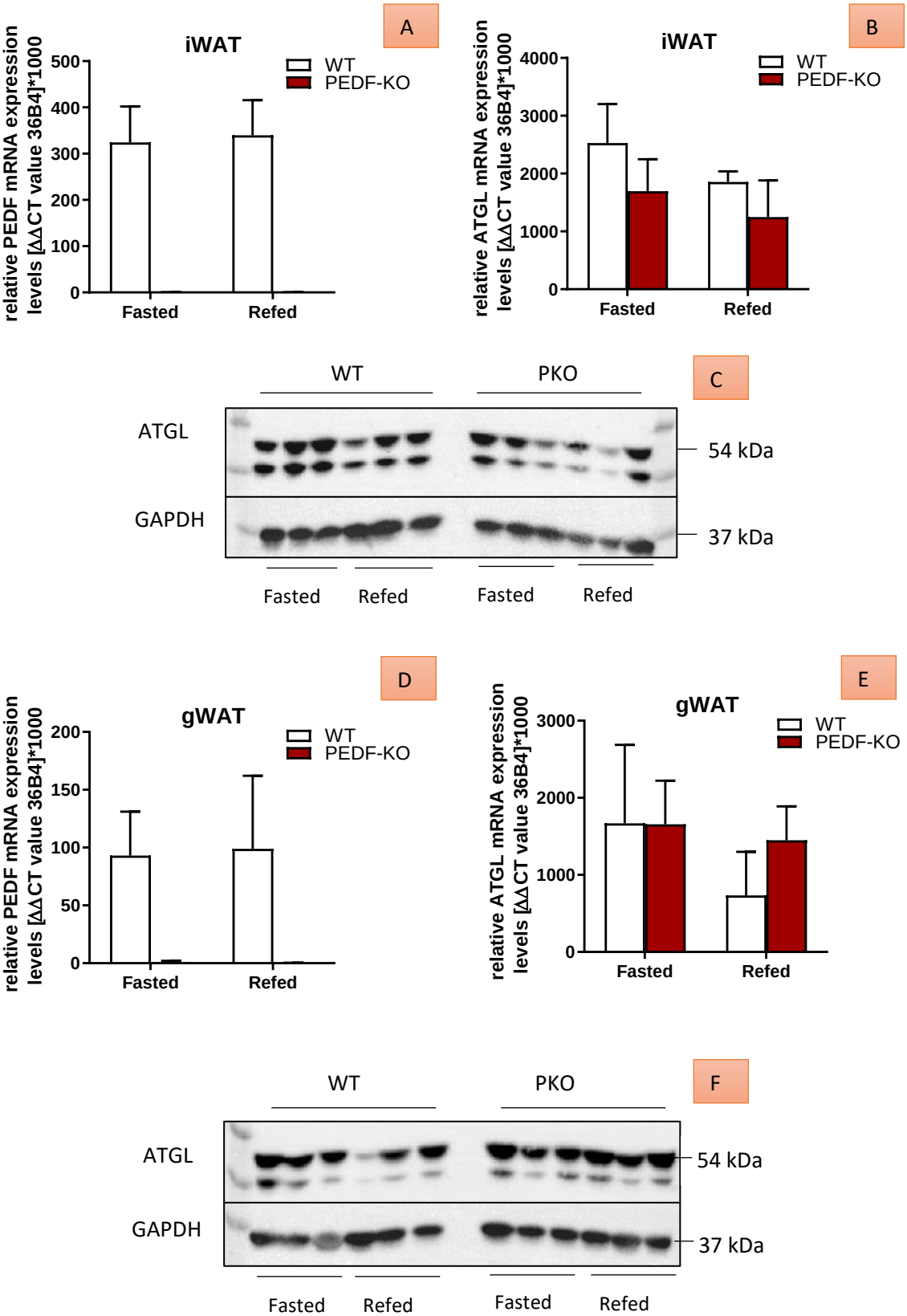

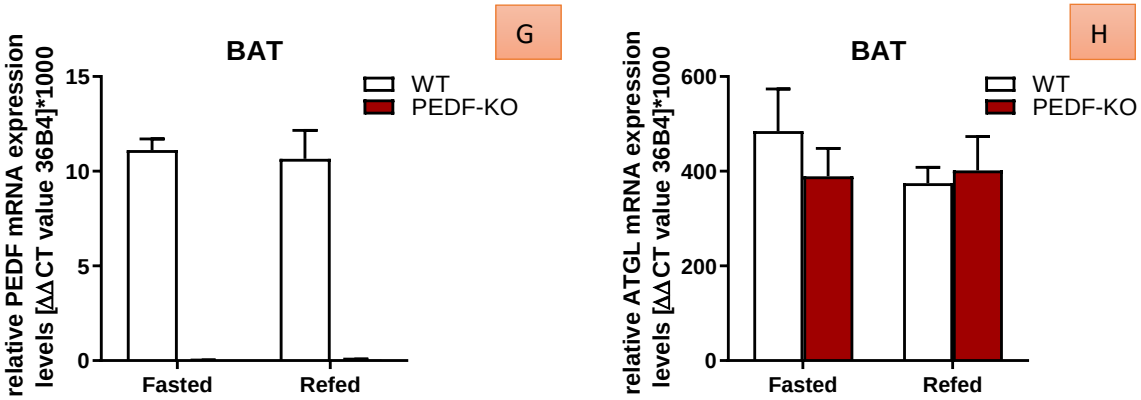

Figure 4.3: mRNA expression levels and protein expression of iWAT, gWAT and BAT of WT and PKO male mice. 14-18 weeks old mice were fasted overnight or fasted overnight and refed for 2 h. mRNA expression levels were analysed using a specific primer pair (PEDF (A,D,G) and ATGL (B,E,H)) using qPCR. Data are shown as mean + standard deviation (n=3). Significance was determined by Student's t-test ($p \leq 0.05$ =*, 0.01=**, 0.001=***). Protein expression analysis (C,F) was performed using 30 µg tissue lysate (1000 g infranatant). This was subjected to SDS PAGE (10% gel) and WB analysis. Specific proteins were detected using ATGL and GAPDH antibodies as well as HRP labelled 2nd antibodies and a Chemidoc System.

mRNA expression of PEDF was not different in the fed and fasted state in iWAT of WT mice. No PEDF mRNA was detected in iWAT, gWAT and BAT of PKO animals verifying the KO-genotype (4.3.A, D, G). As expected, ATGL mRNA expression was reduced (~27%) in iWAT of fed compared to fasted animals. A slight but not significant reduction (33%) in ATGL mRNA expression was observed in PKO compared to WT iWAT. This is reflected by reduced ATGL protein expression in PKO iWAT compared to WT iWAT.

Similar to iWAT, PEDF mRNA expression is not regulated by the feeding status of the mice in gWAT (4.3.D) or in BAT (4.3.G). While there was a clear feeding-fasting effect on ATGL mRNA levels in gWAT and BAT of WT mice (56% reduced in ATGL in refed gWAT, 23% reduced in refed BAT), no feeding-fasting regulation was observed in PKO animals with regard to ATGL mRNA expression in gWAT or BAT (4.3.E,H) and ATGL protein expression in gWAT (4.3.F).

Besides AT, I also investigated ectopic tissues regarding PEDF and ATGL expression.

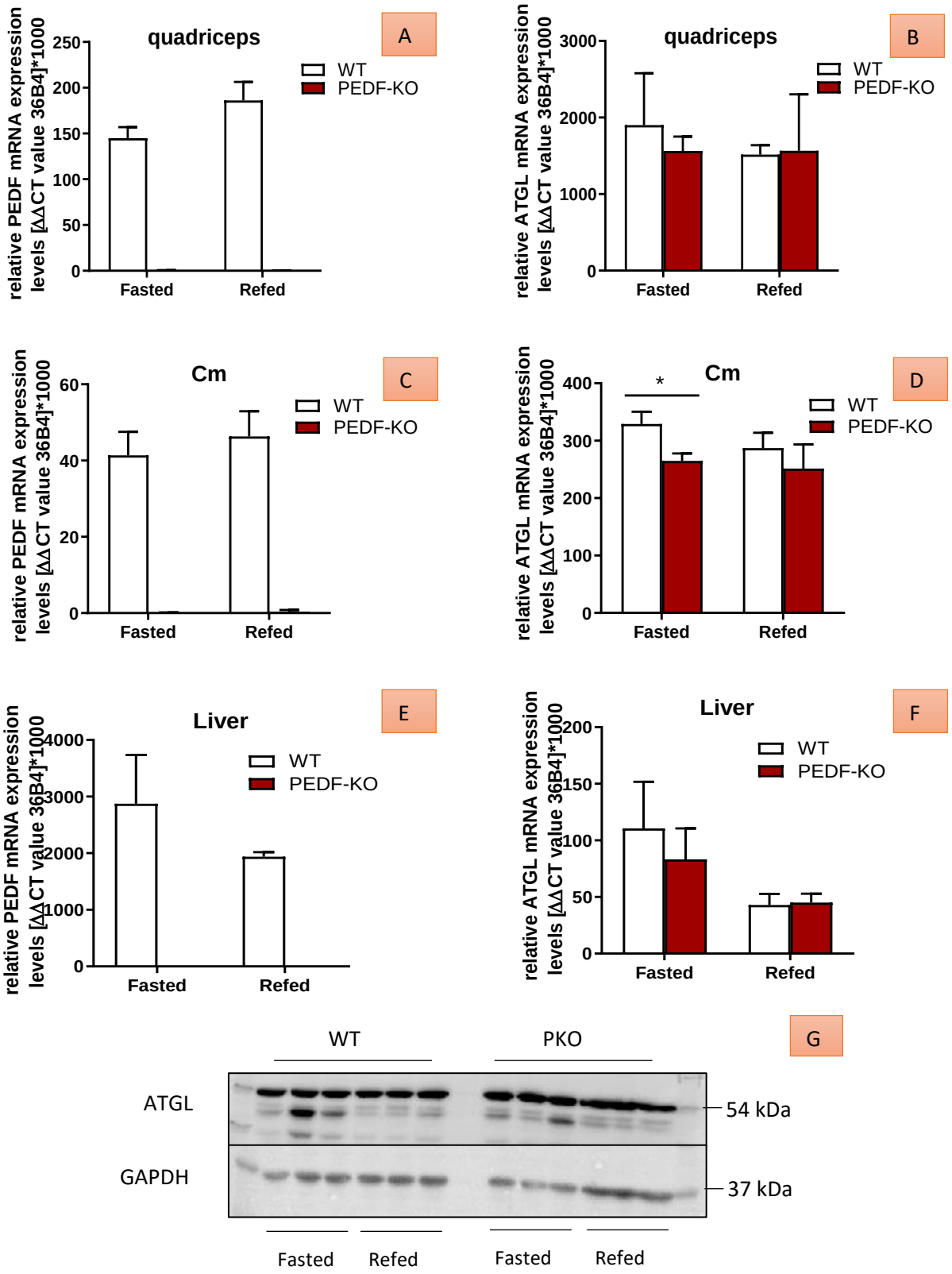

Figure 4.4: mRNA expression levels and protein expression of quadriceps, heart (Cm) and liver of WT and PKO male mice. 14-18 weeks old mice were fasted overnight or fasted overnight and refed for 2 h. mRNA expression levels were analysed using a specific primer pair (PEDF (A, C, E) and ATGL (B, D, F)) using qPCR. Data are shown as mean + standard deviation (n=3). Significance was determined by Student's t-test ($p \leq 0.05$ =*, 0.01=**, 0.001=***). Protein expression analysis (G) was performed using 30 µg tissue lysate (1000 g infranatant). This was subjected to SDS PAGE (10% gel) and WB analysis. Specific proteins were detected using ATGL and GAPDH antibodies as well as HRP labelled 2nd antibodies and a Chemidoc System.

mRNA expression of PEDF was slightly upregulated in the refed skeletal muscle compared to fasted muscle (4.4.A). In the heart, PEDF expression did not differ whereas in the liver PEDF mRNA was downregulated by 33% in the refed compared to the fasted state (4.4.C, E).

No significant differences were observed for mRNA expression of ATGL between fed and fasted skeletal or cardiac muscle (4.4.B, D). PKO animals exhibited 20% reduced ATGL mRNA levels in the fasted heart compared to WT animals (4.4.D). In the liver ATGL mRNA was reduced (61% in WT and 46% in PKO) in refed mice compared to fasted mice (4.4.F). PEDF deficiency did not affect ATGL protein expression (4.4.G).

To investigate whether PEDF deficiency impacts nutrient storage in the liver, I determined liver TG and glycogen concentrations in WT and PKO animals.

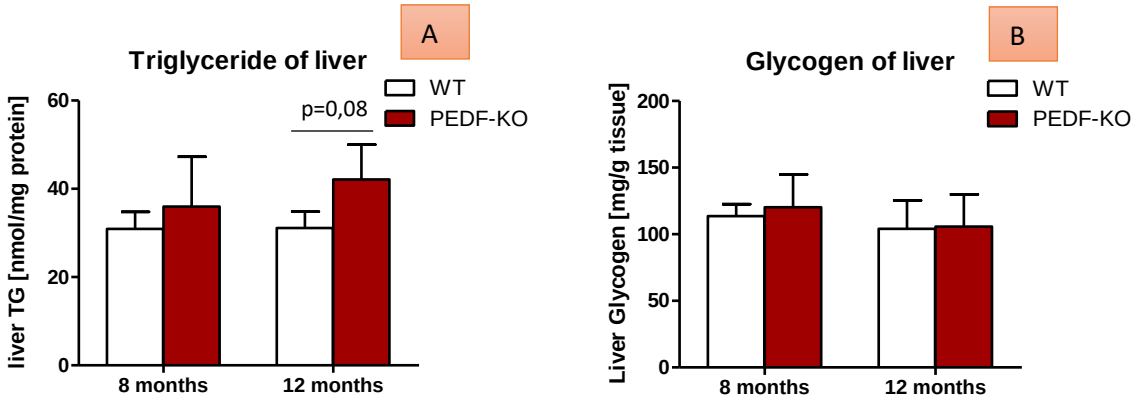

Figure 4.5: **TG and glycogen concentration of livers of WT and PKO male mice** Livers of 8- and 12-months old male mice were extracted using the method of Folch (Chloroform/MeOH 2:1). TG concentration (A) was determined using a comercial kit. TG content is shown relative to protein content, which was determined using BCA reagent and BSA as standard. Free and total glucose content of the same samples were measured using Hexokinase Kit. Glycogen content (B) is shown relative to tissue mass. Data are shown as mean + standard deviation (n=4/5). Significance was determined by Student's t-test (p≤ 0.05 =*, 0.01=**, 0.001=***).

Liver TG content tended to be increased in PKO mice (1.2-fold in 8-months old mice and 1.4-fold in 12-months old mice) compared to WT mice indicating that lipolysis is decreased upon PEDF deficiency. Liver TG content was not different between 8- and 12-months old WT mice. In contrast, TG content of PKO livers increased with age (4.5.A). Glycogen content of liver was not different between WT and PKO mice or between 8- and 12-months old mice (4.5.B).

To verify the results of the enzymatic TG measurement, I also performed TLC analysis of lipid extracts from livers of WT and PKO mice either fed a chow or a HFD.

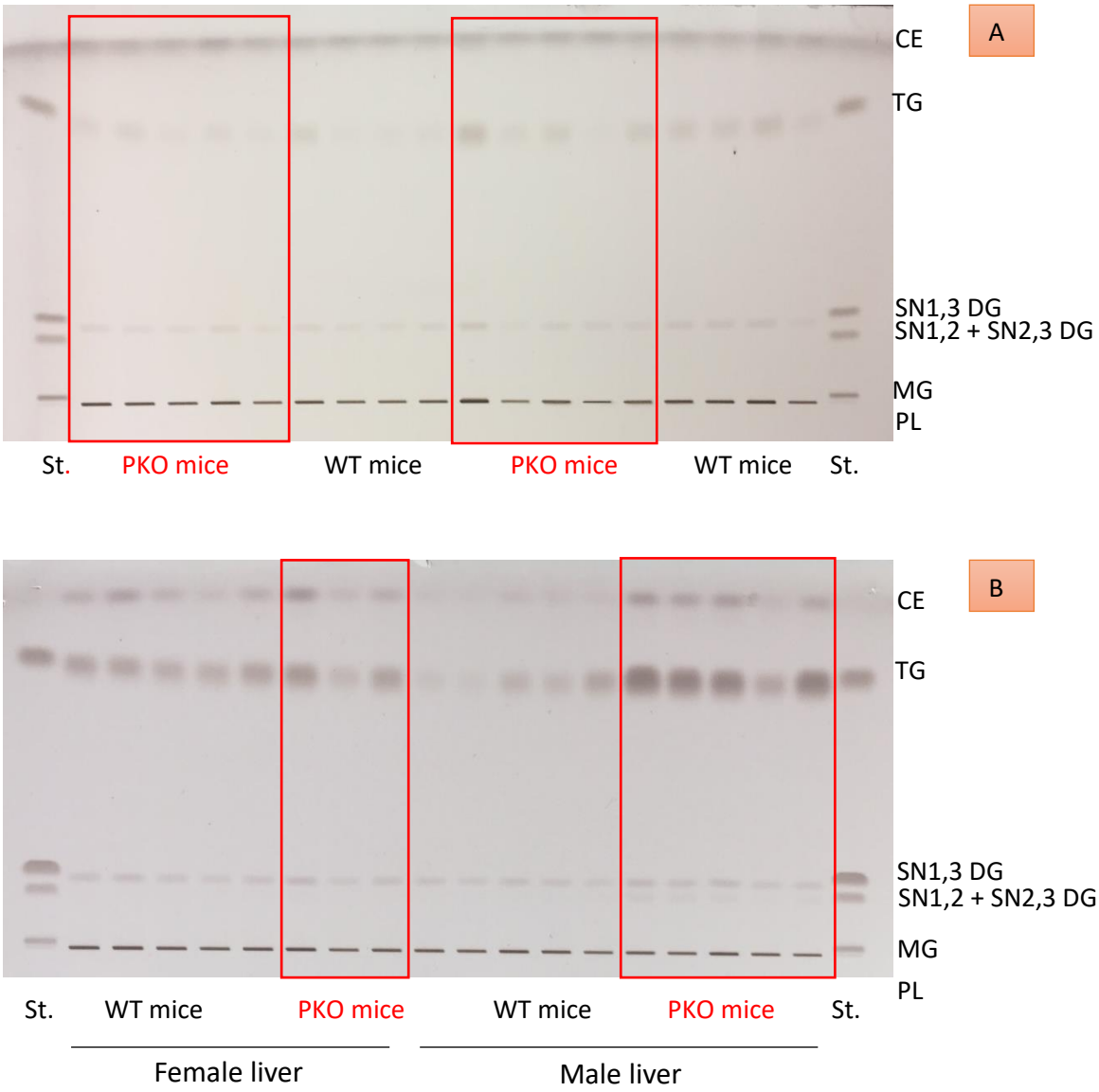

Figure 4.6: TLC of liver extracts of WT and PKO mice on chow diet (A) and on HFD (B). The organic phase extracted of livers of 8- and 12-months old male mice (A) and 10-11 months old female and male mice (B) were diluted 1:4 in chloroform. 5 µl of each sample were applied to TLC and lipids were identified using a mixture of TG, DG and MG as standard and a copper sulphate reagent solvent.

There was no difference in neutral lipid abundance between WT and PKO livers on chow diet (CE, TG, DG, or MG) (4.6.A). However, male PKO mice fed a HFD exhibited an accumulation of CE and TG in their livers compared to WT mice (4.6.B).

Taken together, ATGL levels were feeding-fasting regulated in WT AT and in PKO livers, whereas PEDF levels were only affected by feeding-fasting in muscle and liver of WT mice. Furthermore, aged PEDF deficient mice on chow diet as well as PKO mice on HFD have increased neutral lipid content in the liver.

4.2 PEDF deficiency in the cold

Previous experiments with PKO mice on HFD showed that PKO mice exhibited reduced mitochondrial content and reduced UCP1 expression. To investigate whether PKO mice on chow diet are sensitive to cold exposure, I put the mice in a climate chamber at 5°C and determined body temperature as well as body weight and blood glucose levels.

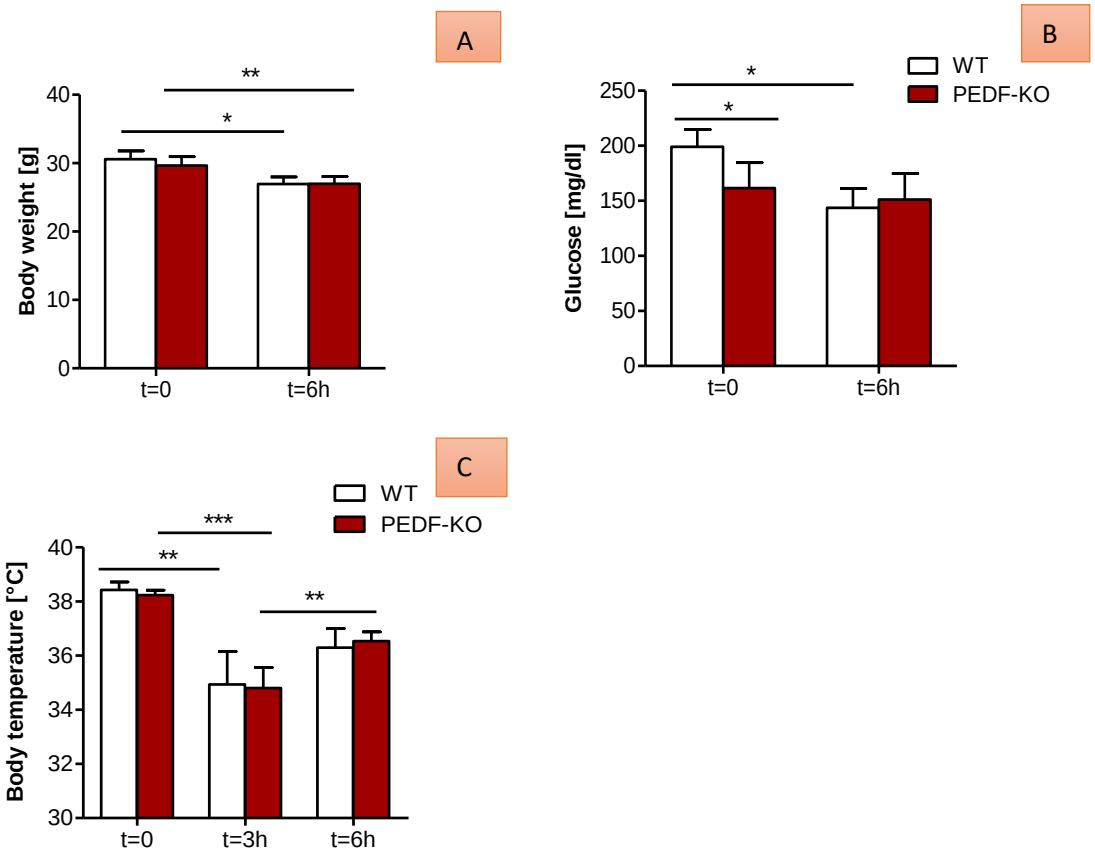

Figure 4.7: **Body weight, -temperature and blood glucose of WT and PKO male mice in the cold.** 13-15 weeks old mice were put at 5°C for 6 h and fasted. Blood glucose (B) was measured using a glucometer. Body weight (A) and -temperature (C) was measured at different timepoints of cold exposure. Data are shown as mean + standard deviation (n=3/6). Significance was determined by Student's t-test (p≤ 0.05 =*, 0.01=**, 0.001=***).

During cold challenge (6 h), all mice lost body weight (-12% WT, -9% PKO mice). Moreover, blood glucose was significantly reduced by 28% in WT mice after 6 h cold exposure. This was

not observed in PKO mice. PKO mice already had 19% reduced blood glucose concentrations at t=0 compared to WT mice. During cold exposure body temperature of WT and PKO mice decreased to the same extent.

I further analysed plasma parameters including FA, glycerol and TG content upon cold exposure.

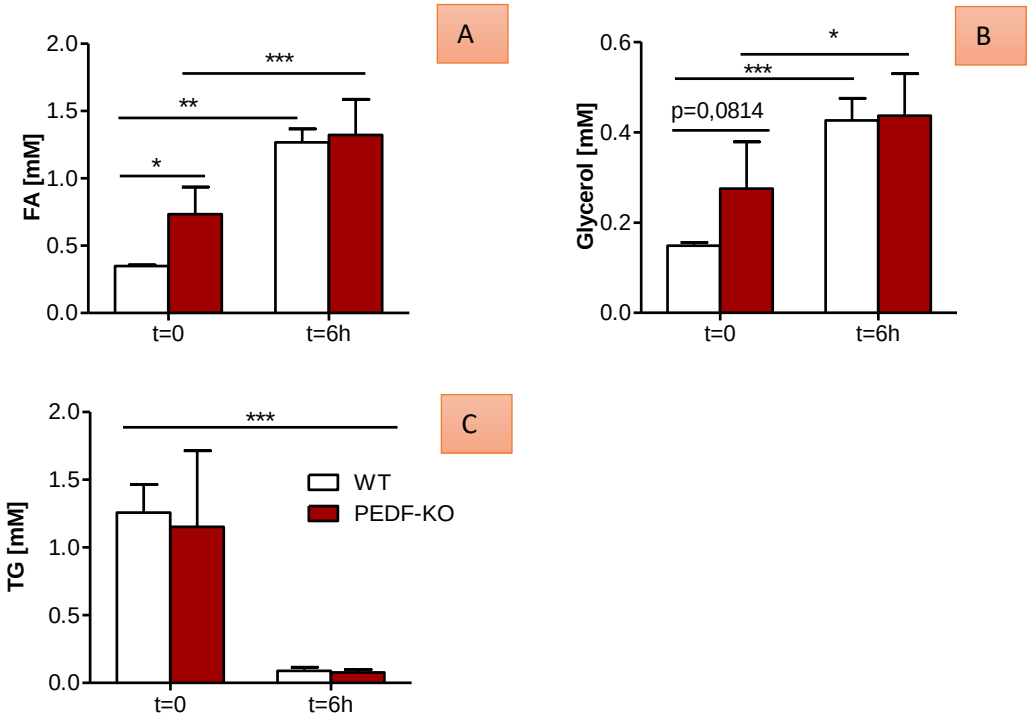

Figure 4.8: Plasma parameters of WT and PKO male mice in the cold. 13-15 weeks old mice were put at 5°C for 6 h and fasted. Then blood was sampled and centrifuged to obtain plasma. FA (A), glycerol (B) and TG content (C) was determined using a comercial colorimetric kit. Data are shown as mean + standard deviation (n=3/6). Significance was determined by Student's t-test (p≤ 0.05 =*, 0.01=**, 0.001=***).

As expected, cold exposure led to an increase of plasma FA and glycerol and to a decrease in plasma TG concentration. This is observed in WT and PKO animals. Interestingly, at timepoint 0 in the ad libitum fed state, PKO mice had increased plasma FA and glycerol concentrations (2-fold) compared to WT mice but same concentrations after 6h cold exposure. Hence, PEDF deficient mice on chow diet can cope with cold temperature.

4.3 Effect of recombinant PEDF on lipolysis in adipocytes

To investigate the effect of PEDF on lipolysis in adipocytes, I first purified recombinant PEDF (rPEDF) from Expi cells using Affinity chromatography.

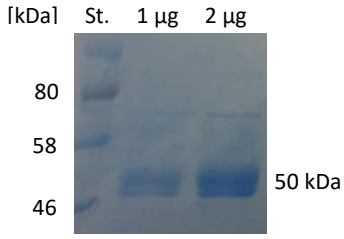

Figure 4.9: Confirmation of purified rPEDF using a 10% SDS gel and Coomassie stain. After protein purification using affinity chromatography, protein concentration was determined. Thereafter, the protein was subjected to a 10% SDS gel and visualized by Coomassie stain.

Fig. 4.9 shows a Coomassie stained SDS gel of the purified protein. Two separate bands corresponding to different degrees of glycosylation are seen.

After differentiation of 3T3-L1 fibroblasts into adipocytes, lipolysis experiments were performed in the presence or absence of TC, Ai, iso and rPEDF.

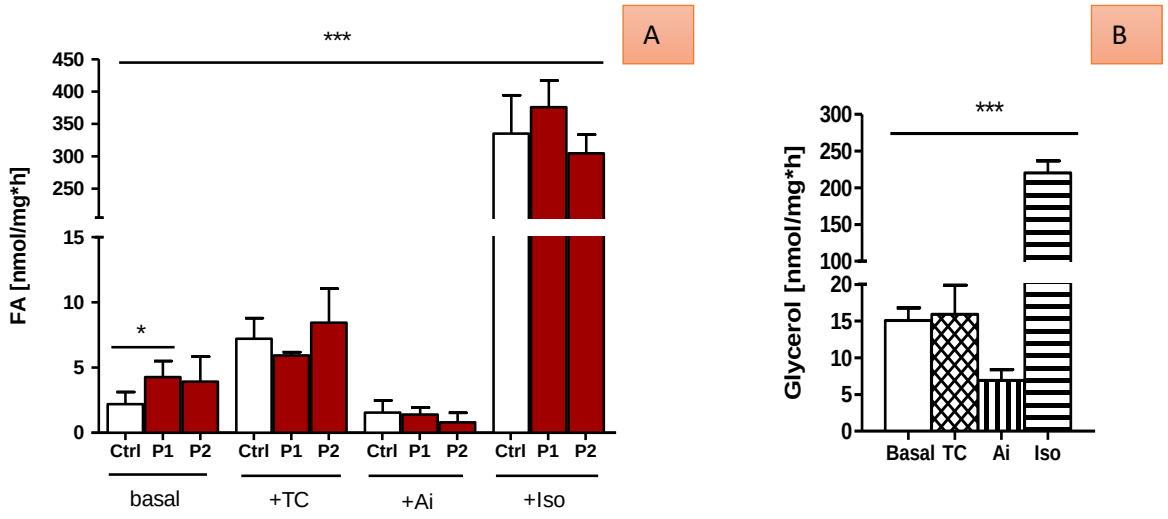

Figure 4.10: FA and glycerol release of 3T3-L1 cells. rPEDF was added to differentiated 3T3-L1 in different concentrations (P1= 1.5 µg/ml, P2= 6 µg/ml). After incubation, basal, Ai inhibited (40 µM) as well as TC (5 µM) and iso stimulated (1 µM) FA (A) and glycerol (B) content was determined. FA and glycerol content is shown relative to protein concentration (mg) and per hour. Data are shown as mean + standard deviation (n=4). Significance was determined by Student's t-test (p≤ 0.05 =*, 0.01=**, 0.001=***).

TC increased the release of FA 3.3-fold, whereas Ai inhibited FA and glycerol release by 30% and 54%, respectively. Iso stimulated FA and glycerol release from adipocytes by 152-fold and 15-fold, respectively. The addition of purified rPEDF at a concentration of 1.5 µg/ml significantly increased FA release (2.2-fold) under basal conditions. No differences in FA release

were observed by rPEDF neither under Ai inhibited nor under iso or TC stimulated conditions.

To exclude that the purification process leads to a non-functional rPEDF protein, I used conditioned medium (CM) from Expi cells to stimulate lipolysis of 3T3-L1 cells.

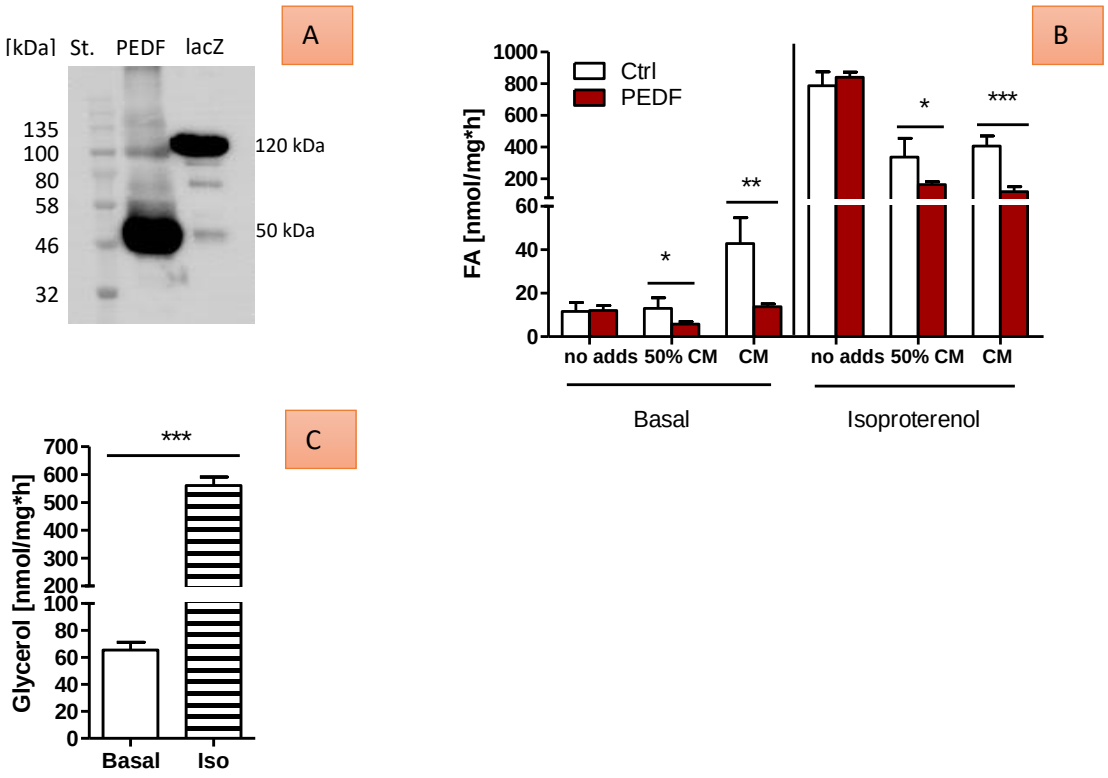

Figure 4.11: A) PEDF protein abundance in CM. B,C) FA and glycerol release of 3T3-L1 cells in the presence of PEDF CM. Expi cells were transfected with Plasmid DNA (C-terminal) PEDF-His or LacZ-His as control. After transfection, medium was collected and WB analysis of 30 µg protein was performed. Proteins were detected using His polyclonal antibody as well as HRP labelled 2nd antibody and a Chemidoc System (A). B) The CM was transferred to differentiated 3T3-L1 in different proportions (50% and 100%). The red bar described as 'no adds' represent the addition of rPEDF (1.5 µg/ml) to 3T3-L1 cells. After incubation 2 h for basal and 1 h for iso stimulation (1 µM), lipolysis was measured as FA and glycerol content in the medium. FA (B) and glycerol (C) content is shown relative to protein concentration (mg) and per hour. Data are shown as mean + standard deviation (n=4). Significance was determined by Student's t-test (p≤ 0.05 =*, 0.01=**, 0.001=***).

Iso stimulated FA and glycerol release 61.8-fold and 8.6-fold, respectively. Unexpectedly addition of CM containing PEDF decreased basal FA release by 56% (50% CM) and by 68% (100% CM). Upon stimulation PEDF CM decreased FA release by 51% (50% CM) and by 71% (100% CM) compared to control CM.

However, I cannot exclude that the CM contained inhibitory molecules that independent of PEDF affect lipolysis. Hence, we switched to a different cell model and stably overexpressed (o/e) PEDF-his (C-term) or LacZ-his (C-term) in OP9K adipocytes (Pia Benedikt). LacZ o/e cells were used as control cells. A polyhistidine tag (6 x His) was cloned on the C- & N-terminus of the gene using the vector pLVX-Tight-Puro (Clontech Laboratories, Inc.). Expression of the gene of interest was under the control of the P_{Tight} promoter (Cloning, Expression and Characterization of PEDF, Pia Benedikt, 2015).

To investigate whether PEDF o/e cells overexpress PEDF, I performed q-RT-PCR on OP9K cells. Therefore, OP9K o/e cells were harvested and RNA was isolated using trizol. mRNA expression was analysed using q-RT-PCR analysis.

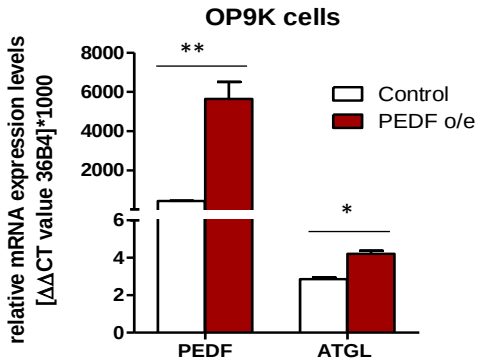

Figure 4.12: PEDF and ATGL mRNA expression levels in LacZ o/e and PEDF o/e OP9K cells. mRNA expression levels were analysed using a specific primer pair (PEDF and ATGL) using qPCR. Data are shown as mean + standard deviation (n=2). Significance was determined by Student's t-test ($p \leq 0.05$ =*, 0.01=**, 0.001=***).

PEDF o/e cells exhibited 10-fold higher PEDF mRNA levels compared to control cells. Hence, I incubated OP9K cells in the presence of CM obtained from control and PEDF o/e OP9K cells. After 2 h basal and 1 h iso stimulated incubation, FA and glycerol content was measured using commercial kits.

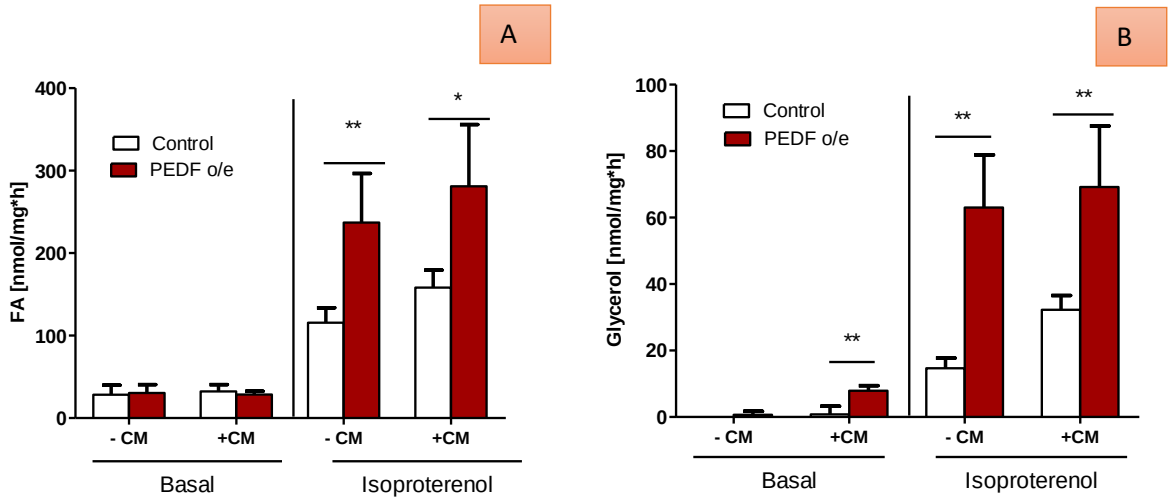

Figure 4.13: FA and glycerol release of LacZ o/e and PEDF o/e OP9K cells. After cells were differentiated, CM was added overnight and next day medium was switched between the cells. As control, cultivation medium was used. After 2 h basal and 1 h iso stimulated incubation (1 µM), lipolysis was measured as FA and glycerol released into the medium. FA (A) and glycerol (B) content is shown relative to protein concentration (mg) and per hour. Data are shown as mean + standard deviation (n=4). Significance was determined by Student's t-test ($p \leq 0.05$ =*, 0.01=**, 0.001=***).

Overexpression of PEDF led to an increase in iso stimulated FA (2.1-fold (-CM), 1.8-fold (+CM)) and glycerol release (4.3-fold (-CM), 2.1-fold (+CM)) as well as basal glycerol release (9.7-fold). However, the addition of medium containing PEDF did not increase the release of lipolytic products.

In another approach, I used CM of Cos7 cells transfected with PEDF or LacZ as control, to stimulate OP9K adipocytes lipolysis. Therefore 0%, 25%, 50%, 100% Cos7 cells CM was incubated 2 h for basal and 1 h for iso stimulated conditions with OP9K adipocytes. Thereafter, FA and glycerol content as a measure of lipolysis were determined.

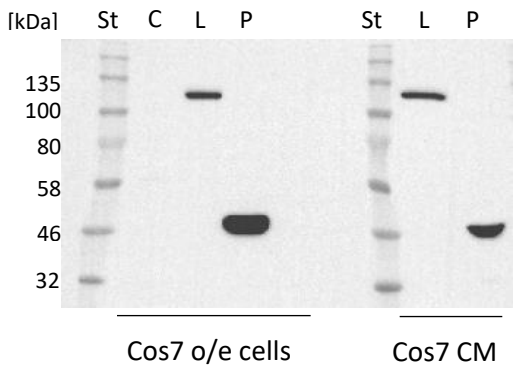

Figure 4.14: Protein expression analysis of Cos7 cells and CM. Cos7 cells were either transfected with LacZ-His or PEDF-His. CM was transferred onto cells the day before experiment. The next day medium was collected as well as cells were disrupted via sonication in 1x PBS. Protein expression analysis was performed using 30 µg cell lysate (1000 g infranatant) and 20 µl of CM. This was subjected to SDS PAGE (10% gel) and WB analysis. LacZ and PEDF protein were detected using His polyclonal antibody as well as HRP labelled 2nd antibody and a Chemidoc System. The abbreviations: St stands for standard, C for control, L for LacZ protein and P for PEDF protein.

WB analysis verified the expression of β-galactosidase (β-gal) and PEDF in Cos7 cells and the secreted protein abundance in the CM.

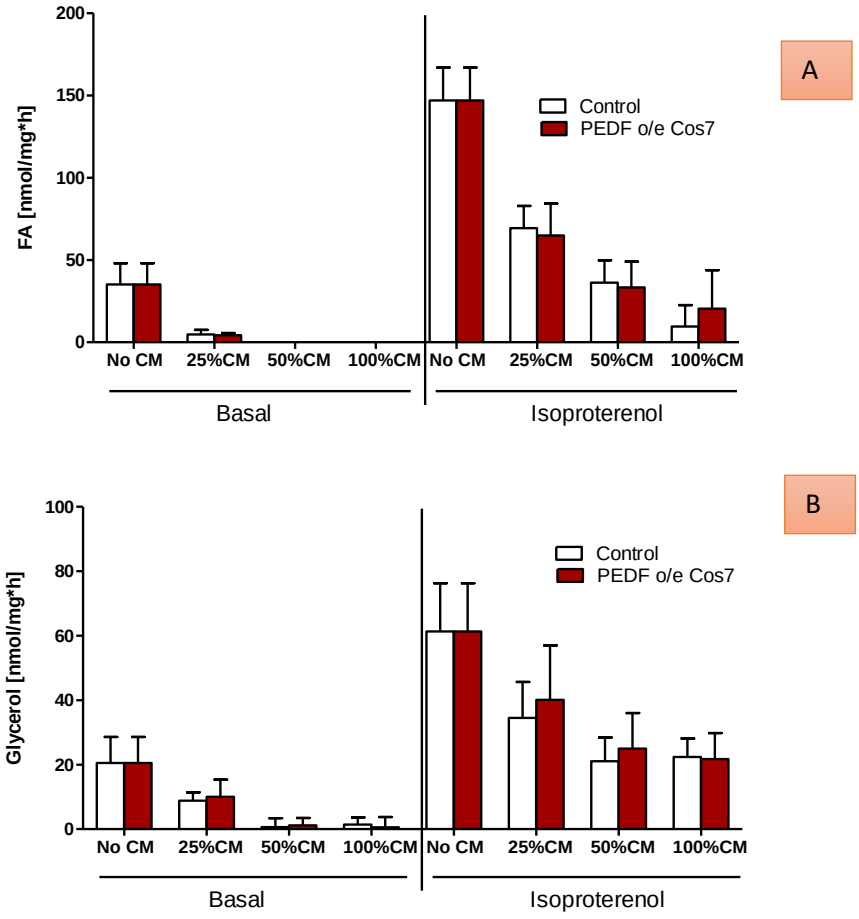

Figure 4.15: FA and glycerol release of OP9K WT cells using CM of Cos7 cells. Cos7 cells were either transfected with LacZ-His or PEDF-His. Medium was put onto Cos7 cells the day before lipolysis experiment. At day of experiment, medium was collected and transferred onto OP9K WT cells in different proportions. After 2 h basal and 1 h iso stimulated incubation (1 µM), lipolysis was measured as FA (A) and glycerol (B) content in the medium. FA and glycerol content is shown relative to protein concentration (mg) and per hour. Data are shown as mean + standard deviation (n=6). Significance was determined by Student's t-test (p≤ 0.05 =*, 0.01=**, 0.001=***).

Although PEDF is highly abundant in the CM, I did not observe a stimulation of lipolysis upon the addition of CM. In contrast, the more CM added to adipocytes, the less was the release of FA and glycerol into the medium independent of the presence of PEDF. This indicates that the CM interferes with lipolysis measurement under these conditions.

Taken together the results using recombinant purified PEDF or PEDF present in CM as well as intracellular overexpression of rPEDF in adipocytes indicate that PEDF does not stimulate lipolysis by an extracellular but by an intracellular mechanism.

4.4 Effect of PEDF deficiency on adipocyte lipolysis

As overexpression of PEDF in OP9K adipocytes increased lipolysis, I next wanted to investigate whether deficiency of PEDF decreases lipolysis in adipocytes. Therefore, I isolated stromal-vascular fraction (SVF) from iWAT of WT and PKO mice. SVF was differentiated to mature adipocytes and lipolysis was measured in the presence and absence of recombinant PEDF and/or iso (4.16.A, B).

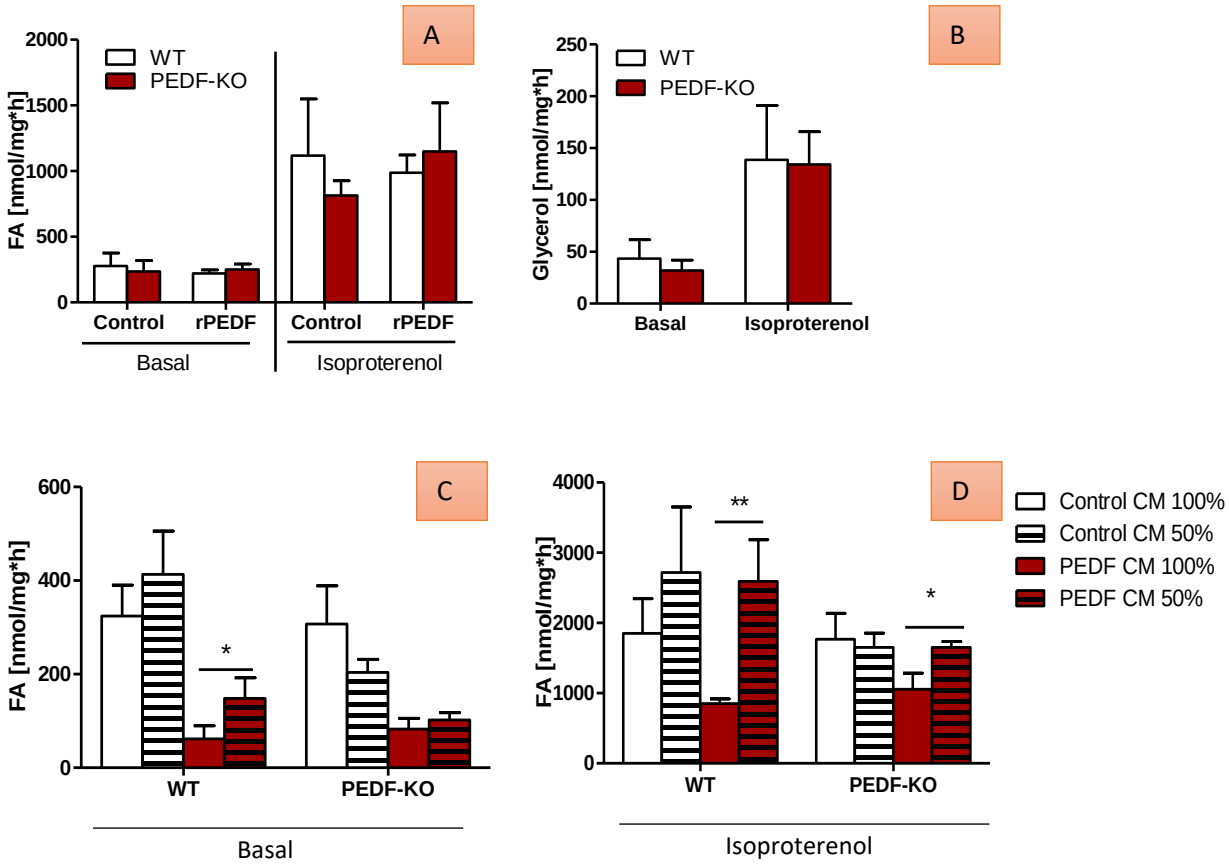

Figure 4.16: **FA and glycerol release of adipocytes from WT and PKO mice.** CM of Expi cells as well as rPEDF (0.75 µg/ml) was incubated with differentiated adipocytes isolated from 10 weeks old female mice. After 2 h basal and 1 h iso stimulated incubation (1 µM), lipolysis was measured as FA and glycerol released into the medium. FA and glycerol content is shown relative to protein concentration (mg) and per hour. Data are shown as mean + standard deviation (n=2/4/6). Significance was determined by Student's t-test (p≤ 0.05 =*, 0.01=**, 0.001=***).

Iso stimulated FA release 4-fold in WT and 3.5-fold in PKO adipocytes, respectively. Stimulated glycerol release was increased 3.2-fold in WT and 4.2-fold in PKO adipocytes, respectively. PKO adipocytes exhibited similar FA and glycerol release under basal and iso stimulated conditions compared to WT adipocytes. The addition of rPEDF did not affect WT adipocyte but slightly increased (1.4-fold) PKO adipocyte FA release under stimulated conditions.

Further, I incubated WT and PKO adipocytes with Expi-cells CM containing rPEDF or β-gal in different concentrations (4.16.C, D). Under basal conditions PEDF-CM reduced FA release by 73% (100% CM) and 64% (50% CM) compared to β-gal-CM in WT adipocytes and by 62% (100% CM) and 50% (50% CM) in PKO adipocytes. Under stimulated conditions PEDF-CM reduced FA release by 54% (100% CM) compared to β-gal-CM in WT adipocytes and by 40% (100% CM) in PKO adipocytes.

To verify whether the same results can be obtained in organ culture, a fat pad assay (see 3.15) was performed. Hence, gWAT of WT and PKO mice was dissected and used for lipolysis experiments (see 3.4).

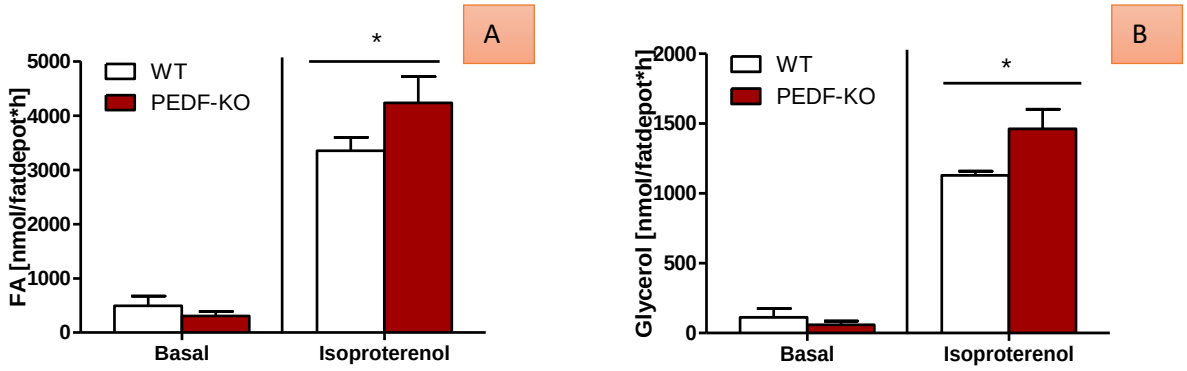

Figure 4.17: FA and glycerol release of gWAT organ cultures of WT and PKO male mice. Fat pads were excised from 13-15 weeks old mice and transferred into 6 well plates containing a cell strainer and medium. After 2 h basal and 1 h iso stimulated incubation (1 µM), lipolysis was measured as FA (A) and glycerol (B) content in the medium. FA and glycerol content is shown relative to fatdepot and per hour. Data are shown as mean + standard deviation (n=3). Significance was determined by Student's t-test (p≤ 0.05 =*, 0.01=**, 0.001=***).

Iso stimulated FA and glycerol release ~8.4-fold in WT and ~19.3-fold in PKO organ cultures, respectively. Under basal conditions fat pads of PKO animals tend to have a reduced release of FA (-37%) and glycerol (-48%) into the medium. Interestingly, the opposite was observed upon lipolytic stimulation. PKO organ cultures released significant more FA (1.26-fold) and glycerol (1.29-fold) into the medium compared to WT organ cultures.

To investigate the effect of PEDF deficiency on TG hydrolysis of AT (iWAT, gWAT, and BAT), a TG-hydrolase activity assay (see 3.8) of dissected AT using radioactively labelled triolein was performed.

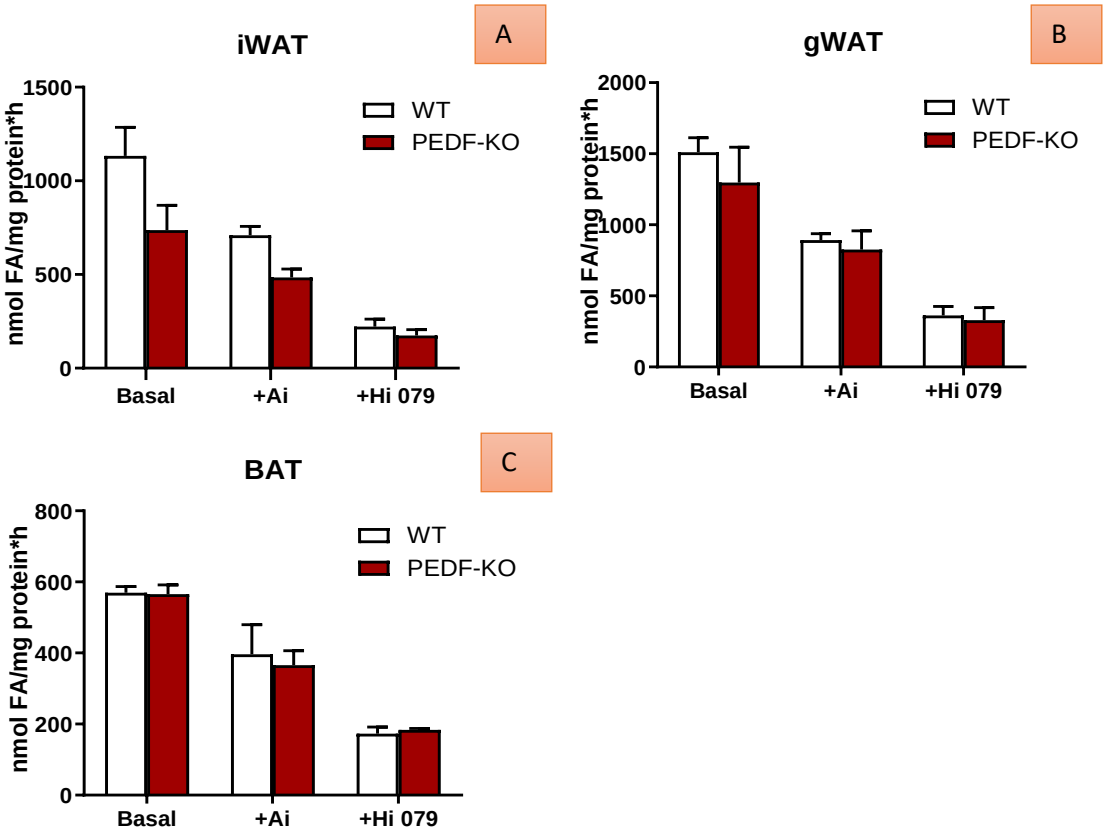

Figure 4.18: **TG-hydrolase activity assay.** iWAT (A), gWAT (B) and BAT (C) of 15 weeks old WT and PKO mice were excised and disrupted in Buffer A. 20 µg lysate protein (16.000 g infranatant) were used for TG-hydrolase assay under basal condition, with 40 µM Ai or with 10 µM Hi-079 addition. After incubation of the samples with radioactively labelled triolein for 1 h at 37°C, radioactively labelled FAs were extracted and measured using liquid scintillation. Data are shown as mean + standard deviation (n=2-3). Significance could not be calculated due to insufficient values.

In TG-hydrolase activity assays using different adipose depots and a radiolabelled TG substrate, I found that PKO iWAT showed 35% less TG-hydrolase activity compared to WT iWAT. Atglistatin (Ai) inhibited TG-hydrolase activity in iWAT (~35%), gWAT (~38%) and BAT (~32%). HSL inhibitor (Hi) reduced TG-hydrolase activity in all adipose depots (iWAT ~78%, gWAT ~75%, BAT ~68%). Lack of PEDF did not affect in vitro TG-hydrolase activity of gWAT or BAT.

Taken together, these results indicate that PEDF deficiency as well as addition of rPEDF to PKO adipocytes moderately affects adipocyte lipolysis upon stimulation. However, addition of medium containing PEDF does not increase lipolytic activity. Furthermore, TG-hydrolysis was slightly reduced in iWAT upon PEDF deficiency.

4.5 Effect of PEDF on adipogenesis

Previous publications suggested an effect of PEDF on the differentiation of adipocytes (Wang et al. 2009). Hence, I determined differentiation of OP9K cells overexpressing PEDF or LacZ. Therefore, I examined neutral lipid accumulation at different time points of differentiation using Oil red O' (4.19.A) and Infinity enzymatic assay (4.19.B).

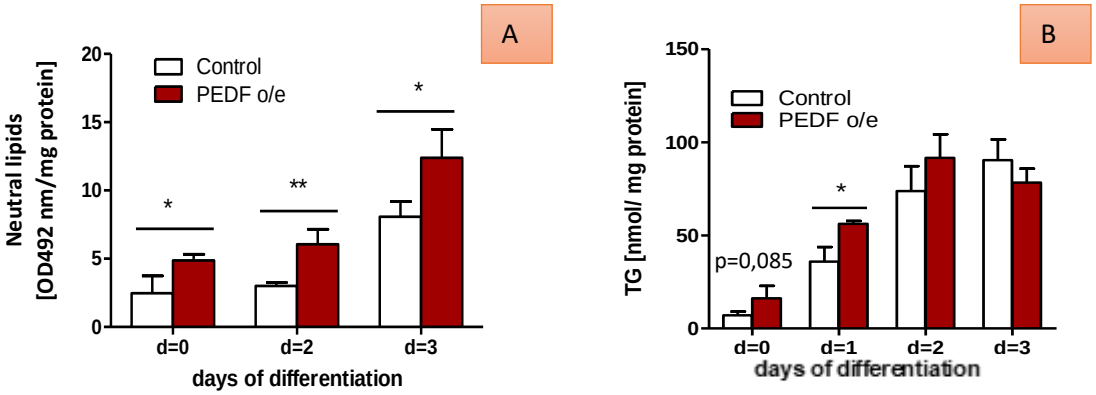

Figure 4.19: Neutral lipid content of LacZ o/e and PEDF o/e OP9K cells. At different timepoints during differentiation cells were stained with Oil red O (A) or TGs were extracted using hexan isopropanol (B). Oil red O' incorporation was measured photometrically. TG content was determined using a comercial colorimetric kit. Results are shown relative to protein concentration (mg). Data are shown as mean + standard deviation (n=3). Significance was determined by Student's t-test (p≤ 0.05 =*, 0.01=**, 0.001=***).

During differentiation, neutral lipid content increased. Oil red O' staining revealed significantly increased (2-fold (d=0,2), 1.5-fold (d=3)) neutral lipid content at all time points in PEDF o/e cells compared to control cells. Interestingly, the increased neutral lipid stain was only partially reflected by increased TG content. While at day 0 and day 1 of differentiation PEDF o/e cells exhibited increased TG content (2.3-fold and 1.6-fold, respectively) compared to control cells; no differences were observed at later time points. This indicates that other lipids besides TG may accumulate in PEDF o/e cells.

To gain more insight into the adipocyte differentiation process in presence or absence of PEDF, I examined differentiation of SVF cells from WT and PKO AT. Therefore, iWAT was dissected and SVF was isolated to obtain preadipocytes. Throughout adipogenesis, cells were analysed every second day using q-RT-PCR analysis.

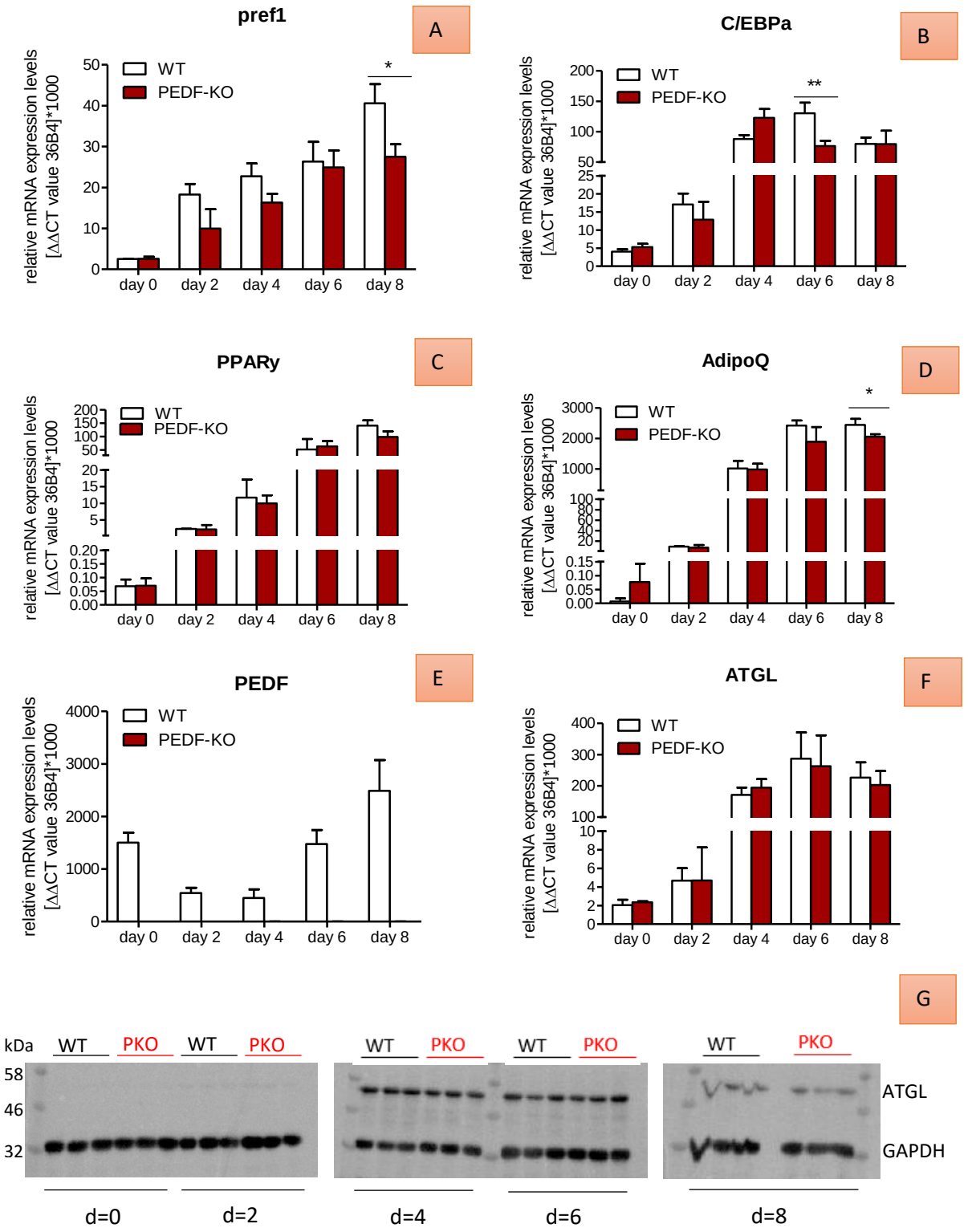

Figure 4.20: Differentiation of iWAT-derived preadipocytes. iWAT was dissected and digested to obtain preadipocytes from 10 weeks old WT and PKO female mice. Differentiation was initiated 2 days post confluent (d=0). Every 2nd day RNA was isolated, and q-RT-PCR was performed to analyse mRNA expression of A) pref1, B) C/EBPa, C) PPARy, D) AdipoQ, E) PEDF and F) ATGL. Data are shown as mean + standard deviation (n=3). Significance was determined by Student's t-test (p≤ 0.05 =*, 0.01=**, 0.001=***). Protein expression analysis (G) was performed using 30 µg cell lysate (12,000 g infranatant). This was subjected to SDS PAGE (10% gel) and WB analysis. Specific proteins were detected using ATGL and GAPDH antibodies as well as HRP labelled 2nd antibodies and a Chemidoc System.

As expected, markers for adipocyte differentiation increased from day 0 to day 8 of differentiation. PKO adipocytes showed slightly reduced mRNA expression of preadipocyte factor 1 (pref1), CCAAT/enhancer binding protein alpha (C/EBPα) and adiponectin (AdipoQ), at days 8, 6, and 8, by 32%, 41%, and 16%, respectively. mRNA expression of peroxisome proliferate activated receptors γ (PPARγ) was not different in PEDF deficient adipocytes compared to WT adipocytes. q-RT-PCR verified that there is no PEDF expression in PKO adipocytes. In WT adipocytes PEDF mRNA levels decreased on day 2 and 4 and increased on day 6 and 8 of adipocyte differentiation. ATGL expression increased during differentiation independent of the presence or absence of PEDF. Similar results were obtained by WB analysis showing an increase of ATGL protein content during adipogenesis in the presence and absence of PEDF.

Together, this indicates that although adipocytes exhibit increased neutral lipid content upon PEDF o/e during adipogenesis, preadipocyte to adipocyte differentiation is not affected by the absence of PEDF. Moreover, neither ATGL mRNA nor protein expression is different in WT and PKO adipocytes during adipocyte differentiation.

5. Discussion

PEDF is a multifunctional protein involved in apoptosis, inflammation, as well as angiogenesis. Previous studies claimed that PEDF has an impact on lipid metabolism and the development of obesity and IR by affecting adipogenesis and lipolysis (Borg et al. 2011, Huang K. et al. 2018a,b). To investigate the role of PEDF in lipid metabolism, I determined body weight, tissue weights, plasma parameters and PEDF and ATGL expression levels in fed and fasted WT and PKO mice. WT and PKO mice weighed the same in the fasted state, whereas in the refed state PKO mice showed significantly increased body weight. Furthermore, PKO mice showed a trend towards increased blood glucose concentration in the refed state. An explanation for this could be an increased food intake of PKO mice. Therefore, in future experiments food intake should be included in the measurements.
In WT mice, fasting led to a reduction in AT depots, which is explained by increased lipolysis providing substrates for oxidative tissues. Interestingly, PKO mice did not reduce their gWAT weight in response to fasting indicating defective lipid mobilization in this tissue. Reduced lipid mobilization from AT would result in reduced abundance of lipolytic products in the circulation. However, plasma concentrations for FA and glycerol from PKO mice did not differ from WT mice. Controversy to my data, Dai et al. (2013a) described increased FA and glycerol levels in plasma upon prolonged PEDF administration, suggesting that PEDF enhances lipolysis.

Besides fasting, lipolysis is also activated in response to cold to provide substrate for BAT thermogenesis. Hence, I wanted to investigate PEDFs role in thermogenesis. Preliminary data (Martina Schweiger) showed a decrease in UCP1 expression and an increase in sensitivity to cold in PKO mice on HFD. Therefore, I performed a cold exposure experiment with WT and PKO mice on chow diet. PKO mice on chow diet did not show a higher sensitivity to cold than WT mice. Though, in the ad libitum fed state (t=0), PKO mice showed reduced blood glucose concentrations, which did not further decrease upon cold exposure compared to WT mice. Cold exposure reduced plasma TG and increased AT lipolytic products in plasma of both genotypes. However, PEDF deficient mice showed reduced mobilization of FA and glycerol upon cold exposure.

To further investigate whether lipid mobilization is reduced in gWAT of PKO animals I performed fat pad assays. Indeed, basal lipolysis was slightly decreased in PKO animals com-

pared to WT animals. This was in accordance with results obtained by in vitro TG-hydrolase activity assays, where iWAT showed significantly less activity in PKO compared to WT mice. However, in this experiment gWAT TG-hydrolase activity was comparable between the genotypes. In line with studies performed by Borg et al. (2011) using fat pads; I also found that PEDF is not important for stimulated lipolysis. In contrast, I even found increased release of FA from stimulated PKO AT organ explants compared to WT AT organ explants.

To analyse whether PEDF influences mobilization of FA in vitro, I investigated whether purified murine recombinant PEDF affects 3T3 adipocyte and primary adipocyte lipolysis. Basal lipolysis was slightly increased in the presence of 1.5 µg/ml rPEDF. However, addition of murine rPEDF did not significantly increase the release of lipolytic products in primary adipocytes. Though, Crowe et al. (2009) showed that addition of human rPEDF to cultured 3T3-L1 adipocytes as well as administration of PEDF to mice significantly stimulates lipolysis. The discrepancy to my results could be due to a dysfunctional protein or that only human protein affects lipolysis. To exclude that the purification process led to a non-functional rPEDF protein, I added CM of PEDF o/e cells to 3T3 adipocytes in order to perform lipolysis experiments. However, addition of medium containing PEDF did not increase lipolytic products neither under basal nor under stimulated conditions.

As my studies using rPEDF indicate that extracellular PEDF does not significantly increase adipocyte lipolysis, I wanted to study the intracellular role of PEDF on lipolysis. Therefore, OP9K cells were lentiviral infected with a plasmid to stably overexpress PEDF. After β-adrenergic stimulation, PEDF o/e cells showed elevated release of lipolytic products whereas again the addition of medium containing PEDF did neither increase FA release nor glycerol release. This strengthens the hypothesis that PEDF has an intracellular function on lipolysis.

PEDF has been shown to potentially regulate lipolysis by interfering with ATGL protein abundance (Dai et al. 2013a, Borg et al. 2011, Notari et al. 2006). The amount of protein is determined by transcription, translation, as well as by degradation. Hence, I first looked whether ATGL mRNA and protein expression is affected by the absence of PEDF. Therefore, I performed WB and q-RT-PCR analysis on WT and PEDF deficient tissues. PEDF mRNA expression levels were not regulated by feeding-fasting in AT. However, upon refeeding PEDF levels

were increased in muscle and decreased in liver. In line with previous publications (Kershaw et al. 2006), mRNA levels of ATGL were increased by fasting and reduced by feeding in WT AT. Though in PKO AT, ATGL expressions were not different between the fed and fasted state. A possible explanation might be an interference of PEDF with insulin action as addition of insulin negatively regulates ATGL in a dose dependent manner (Kershaw et al. 2006). Another explanation could be that PEDF affects fasting-induced glucocorticoid release, which affects ATGL levels (Zechner et al. 2005, Villena et al. 2004). However, in the liver ATGL expression is not affected by PEDF deficiency.

A study by Chung et al (2008) showed that PEDF deficiency causes liver steatosis. To investigate whether this is also observed in our PKO mice, I determined liver lipid content. Young mice did not display TG accumulation however aged PKO mice showed a clear trend towards increased liver TG content compared to WT mice. This effect was more pronounced on a HFD where TG as well as CE significantly accumulated in PKO livers. This indicates that liver steatosis in PKO mice is a slowly occurring process with age or with high caloric intake. It can be suggested that increased TG content results from reduced lipolysis in PKO livers (Chung et al. 2008, Dai et al. 2013b). Alternatively, increased lipid content may also derive from increased de novo lipogenesis, increased FA uptake or reduced lipoprotein secretion. Further studies are needed to clarify TG accumulation in PKO livers.

Previous studies have shown that recombinant PEDF influences adipogenesis (Wang et al. 2009, Huang K. et al. 2018b). Therefore, I investigated PEDFs role on differentiation of adipocytes. Adipogenesis is the differentiation process of preadipocytes to mature adipocytes. It is induced by the transcription factors C/EBPα as well as PPARγ leading to an activation of adipocyte specific genes like AdipoQ (Huang K. et al. 2018b). In my experiments I analysed adipocyte markers such as C/EBPα, PPARγ and AdipoQ in WT and PKO mice. During differentiation, all markers increased independent on the genotype. This indicates that probably only exogenously added PEDF but not PEDF deficiency influences adipogenesis.
To identify undifferentiated adipocytes, pref1 marker was analysed. Although Wang et al. (2009) claimed that PEDF as well as pref1 expression is decreased in mature adipocytes, in my experiments I observed a decrease of PEDF expression on early days of differentiation followed by an increase on later stages of adipogenesis; as well as increased pref1 expres-

sion over time of differentiation. Even though the cells had the shape of adipocytes, the unexpected increase of pref1 marker in WT and PKO mice might indicate incompletely differentiated adipocytes. Moreover, ATGL gradually increased during adipogenesis. This fits with data published by Huang K. et al. (2018b). However, no differences in ATGL mRNA or protein between WT and PKO adipocytes were observed indicating that PEDF deficiency does not alter ATGL expression. However, Dai et al. (2013a) described an increase of ATGL protein expression by knocking down PEDF in 3T3-L1 adipocytes. A possible explanation for this discrepancy could be that in my experiments I used primary adipocytes of PKO mice instead of 3T3-L1 adipocytes. To investigate whether PEDF overexpression affects differentiation, I examined neutral lipid accumulation in PEDF or LacZ o/e OP9K cells during adipogenesis. Overexpression of PEDF increased total neutral lipid content in OP9K cells during differentiation, whereas TG content was only moderately increased. However, PEDF is shown to have liver TG reducing effects when administered to mice (Kawaguchi et al. 2010). This indicates that besides TG, other neutral lipids like CE accumulate upon PEDF o/e in OP9K cells.

Taken together, there are still inconsistencies regarding PEDF in lipolysis. My studies showed a slight increase in lipolysis in intact adipocytes but no direct effect on TG hydrolysis. Additionally, plasma parameters on feeding-fasting experiment as well as upon cold exposure were not altered in PKO mice compared to WT mice. Furthermore, PEDF deficiency did neither affect adipogenesis nor ATGL protein expression. Overall my findings question a prominent role for PEDF in lipolysis. Thus, more experiments must be performed in order to clarify whether PEDF is important in the regulation of lipolysis or whether it has, to a certain extent, a non-essential regulatory function.

I. Abbreviations

Table I: Abbreviation list

aa	Amino acids
AC	Adenylate cyclase
AdipoQ	Adiponectin
Ai	Atglistatin
amp	Ampicillin
AT	Adipose tissue
ATP	Adenosine triphosphate
ATGL	Adipose triglyceride lipase
β-AR	β-adrenergic receptor
β-gal	β-galactosidase
BAT	Brown adipose tissue
BCA	Bicinchoninic acid
BSA	Bovine serum albumin
C/EBPa	CCAAT/enhancer binding protein alpha
cAMP	Cyclic adenosine monophosphate
cDNA	Complementary DNA
CE	Cholesteryl ester
CGI-58	Comparative gene identification protein 58
Cm	Cardiac muscle or heart
CM	Conditioned medium
Cpm	Counts per minute
ddH_2O	Distilled, deionized water
DEPC	Diethyl pyrocarbonate
DG	Diglyceride
DMEM	Dulbeccos modified eagle medium
DMSO	Dimethylsulfoxide
EDTA	Ethylenediaminetetraacetic acid
Egr	Early growth response protein

FA	Fatty acid
FCS	Fetal calf serum
FoxO1	Forkhead transkription factor 1
fw	Forward
GAPDH	Glycerinaldehyd-3-phosphat-Dehydrogenase
gWAT/ iWAT	Gonadal WAT/ inguinal WAT
HFD	High fat diet
Hi	HSL inhibitor
HSL	Hormone-sensitive lipase
IBMX	3-Isobutyl-1-methylxanthin
IR	Insulin resistance
IRS	Insulin receptor substrate
Iso	Isoproterenol
kDa	Kilo Dalton
LPL	Lipoprotein lipase
Memα	Minimum essential medium α
MG	Monoglyceride
MGL	Monoglyceride lipase
n.f.	Nuclease free
o/e	Overexpressing
ORO	Oil red O’
p.a.	Pro analysi
PBS	Phosphate buffered saline
PC	Phosphatidyl choline
PD	Patatin domain
PDE3B	Phosphodiesterase 3B
PEDF	Pigment epithelium derived factor
PI	Phosphatidyl inositol
PI3	Phosphatidylinositol-3-kinase
PKA	Protein kinase A
PKO or PEDF-KO	PEDF- knockout

PL	Phospholipids
PPARγ	Peroxisome proliferate activated receptors γ
Pref1	Preadipocyte factor 1
PS	Penicillin-Streptomycin
PVDF	Poly vinylidene fluorid
qPCR	Quantitative polymerase chain reaction
RCL	Reactive central loop
RE	Retinyl esters
rev	Reverse
RIPA	Radio immuno precipitation assay buffer
rPEDF	Recombinant PEDF
RT	Room temperature
SDS-PAGE	Sodium-Dodecyl sulfate-polyacrylamide gel electrophoresis
SVF	Stromal-vascular fraction
TC	Triacsin C
TG	Triglyceride
TLC	Thin layer chromatography
UCP1	Uncoupling protein 1
VEGF	Vascular endothelial growth factor
WAT	White adipose tissue
WB	Western Blot
WT	Wild type

II. References

Bal, N.C. et al., 2017. Mild cold induced thermogenesis: are BAT and skeletal muscle synergistic partners. *Department of Physiology and Cell Biology*. p. 1.

Becerra, S. P. & Notario, V., 2013. The effects of PEDF on cancer biology: mechanisms of action and therapeutic potential. *Nature Reviews Cancer.* p. 259.

Benedikt, P. 2015. Cloning, Expression and Characterization of PEDF. *Master thesis*. pp. 34-35.

Borg, M. L. et al., 2011. Pigment Epithelium–Derived Factor Regulates Lipid Metabolism via Adipose Triglyceride Lipase. *Diabetes Journals*. pp. 1458-1465.

Carnagarin, R. et al., 2015. PEDF-induced alteration of metabolism leading to insulin resistance. *Molecular and Cellular Endocrinology*. pp. 98-103.

Chakrabarti, P. et al., 2011. SIRT1 controls lipolysis in adipocytes via FOXO1-mediated expression of ATGL. *Journal of Lipid Research*. pp. 1693–1699.

Chakrabarti, P. et al., 2013. Insulin Inhibits Lipolysis in Adipocytes via the Evolutionarily Conserved mTORC1-Egr1-ATGL-Mediated Pathway. *Molecular and Cellular Biology*. pp. 3659-3663.

Chung, C. et al., 2008. Anti-angiogenic pigment epithelium-derived factor regulates hepatocyte triglyceride content through adipose triglyceride lipase (ATGL). *Journal of Hepatology*. pp. 471, 476.

Coelho, M. et al.,2012. Biochemistry of adipose tissue: an endocrine organ. *Archives of Medical Science*. pp. 191-193

Cos-7 cells. *Thermo Fisher Scientific.* Available at: https://www.thermofisher.com/at/en/home/technical-resources/cell-lines/c/cell-lines-detail-5.html. [Accessed July 17.2019].

Crowe, S., 2009. Pigment Epithelium-Derived Factor Contributes to Insulin Resistance in Obesity. *Cell Metabolism.* pp. 40, 44.

Czech, M., 2017. Insulin action and resistance in obesity and type 2 diabetes. *Nature Medicine.* p. 804.

Dai, Z. et al., 2013a. Dual regulation of adipose triglyceride lipase by pigment epithelium-derived factor: A novel mechanistic insight into progressive obesity. *Molecular and Cellular Endocrinology*. pp. 123–134.

Dai, Z. et al., 2013b. Intracellular pigment epithelium-derived factor contributes to triglyceride degradation. *International Journal of Biochemistry and Cell Biology*. p. 2076.

Dechandt, CRP. et al., 2017. Triacsin C reduces lipid droplet formation and induces mitochondrial biogenesis in primary rat hepatocytes. *Journal of bioenergetics and biomembranes*. Available at: https://www.ncbi.nlm.nih.gov/pubmed/28918598 [Accessed July 17.2019].

Djalalinia, S. et al., 2015. Health impacts of obesity. *Pakistan Journal of Medical Sciences*. pp. 239-241.

Duh, E.J., 2002. Pigment Epithelium-Derived Factor Suppresses Ischemia-Induced Retinal Neovascularization and VEGF-Induced Migration and Growth. *Investigative Ophtalmology and visual science*. p. 821.

Duncan R. et al., 2007. Regulation of Lipolysis in adipocytes. *Annual Review of Nutrition*. pp. 1-6.

Fernandez-Garcia, N.I. et al., 2007. Pigment epithelium-derived factor as a multifunctional antitumor factor. *Journal of molecular medicine*. pp. 15, 18-20.

Granneman, J. et al., 2007. Analysis of lipolytic protein trafficking and interactions in adipocytes. Journal of Biological Chemistry. pp. 5726-5727.

Guo, S., 2014. Insulin signaling, resistance, and metabolic syndrome: insights from mouse models into disease mechanisms. *Journal of Endocrinology.* pp. T1-T2, T8.

Haemmerle, G. et al., 2002. Hormone-sensitive Lipase Deficiency in Mice Causes Diglyceride Accumulation in Adipose Tissue, Muscle, and Testis. *The Journal of Biochemical Chemistry.* p. 4806.

Haemmerle, G. et al., 2006. Defective Lipolysis and Altered Energy Metabolism in Mice Lacking Adipose Triglyceride Lipase. *Science New York.* p. 736.

Hardy, T.O. et al., 2014. What causes the insulin resistance underlying obesity? *Current Opinion in Endocrinology, Diabetes and Obesity*. pp. 2,6-7.

He, X. et al., 2015. PEDF and its roles in physiological and pathological conditions: implication in diabetic and hypoxia-induced angiogenic diseases. *Clinical Science*. pp. 806-808; 813.

Hopper, C., Overview of insulin signaling pathways. Available at: https://www.abcam.com/pathways/overview-of-insulin-signaling-pathways. [Accessed September 17.2019]

Huang, K.T. et al., 2018a. Pigment epithelium-derived factor in lipid metabolic disorders. *Biomedical Journal*. pp. 104-105.

Huang, K.T. et al., 2018b. Decreased PEDF expression promotes adipogenic differentiation through the upregulation of CD36. *International Journal of Molecular Sciences.* pp. 9-10.

Huang, M. et al., 2018. Pigment Epithelium-Derived Factor Plays a Role in Alzheimer's Disease by Negatively Regulating Aβ42. Neurotherapeutics. pp. 728, 739.

Jaworski, K. et al. 2007. Regulation of Triglyceride Metabolism. IV. Hormonal regulation of lipolysis in adipose tissue. *American Journal of Physiology-Gastrointestinal and Liver Physiology*. pp. G3–G4.

Kawaguchi, T. et al., 2010. Structure-Function Relationships of PEDF. *Current Molecular Medicine.* p. 308.

Kershaw, EE. & Flier, J., 2004. Adipose tissue as an endocrine organ. *Journal of Clinical Endocrinology and Metabolism*. p. 2548.

Kershaw, EE. et al., 2006. Adipose Triglyceride Lipase. *Diabetes.* pp. 148, 156.

Klingenspor, M., 2003. Cold-induced recruitment of brown adipose tissue thermogenesis. *Experimental physiology*. p. 142.

Lane, J.M. et al., 2014. Development of an OP9 derived cell line as a robust model to rapidly study adipocyte differentiation. *Plos One Journal.*
Available at: https://paperity.org/p/60310246/development-of-an-op9-derived-cell-line-as-a-robust-model-to-rapidly-study-adipocyte. [Accessed July 17. 2019].

Langin, D. 2006. Adipose tissue lipolysis as a metabolic pathway to define pharmacological strategies against obesity and the metabolic syndrome. *Pharmacological research.* p. 484. Available at: https://www.ncbi.nlm.nih.gov/pubmed/16644234. [Accessed August 02.2019].

Lass, A. et al., 2006. Adipose triglyceride lipase-mediated lipolysis of cellular fat stores is activated by CGI-58 and defective in Chanarin-Dorfman Syndrome. *Cell Metabolism*. pp. 309-310.

Lass, A. et al., 2011. Lipolysis – A highly regulated multi-enzyme complex mediates the catabolism of cellular fat stores. *Progress in lipid research*. pp. 14-17.

Li, Z. et al., 1994. Isolation and characterization of the gene for mouse hormone-sensitive lipase. *Genomics*. p. 259.

Mayer, N. et al., 2014. Development of small molecule inhibitors targeting adipose triglyceride lipase. *Nature chemical biology*. p. 4.

Morrison, L. & McGee, S.L., 2015. 3T3-L1 adipocytes display phenotypic characteristics of multiple adipocyte lineages. *Journal Adipocyte.* Available at: https://www.ncbi.nlm.nih.gov/pmc/articles/PMC4573194/. [Accessed July 17. 2019].

Notari, L. et al., 2006. Identification of a Lipase-linked Cell Membrane Receptor for Pigment Epithelium-derived Factor. *Journal of biological chemistry*. pp. 38022, 38033-38036.

Niyogi, S. et al., 2019. PEDF promotes nuclear degradation of ATGL through COP1. *Biochemical and Biophysical Research Communications.* pp. 1,6.

Rassow, J. et al., 2012. Duale Reihe Biochemie. 3. Auflage. *Thieme*. pp. 221-225.

Silva, K.R. et al., 2017. Characterization of stromal vascular fraction and adipose stem cells from subcutaneous, preperitoneal and visceral morbidly obese human adipose tissue depots. *Plus One Journal.* Available at: https://www.ncbi.nlm.nih.gov/pmc/articles/PMC5360317/. [Accessed July 17. 2019].

SSNIFF Diets. http://www.ssniff.com/index.php. [Accessed September 15.2019].

Thermo Fisher Scientific. Expi293F™ Cells. Available at: https://www.thermofisher.com/order/catalog/product/A14527. [Accessed July 25.2019].

U.S. National Library of Medicine-Pubchem. Isoproterenol. Available at: https://pubchem.ncbi.nlm.nih.gov/compound/Isoproterenol. [Accessed August 01. 2019].

Villena, J. et al., 2004. Desnutrin, an adipocyte gene encoding a novel patatin domain-containing protein, is induced by fasting and glucocorticoids: Ectopic expression of desnutrin increases triglyceride hydrolysis. *Journal of Biological Chemistry*. pp. 47066, 47071.

Voet, D.J. et al., 2008. Principles of Biochemistry. 3rd Edition. Student version. *John Wiley and Sohn. Inc*. pp. 677-683.

Vujic, N. et al., 2017. Monoglyceride lipase deficiency affects hepatic cholesterol metabolism and lipid-dependent gut transit in ApoE-/- mice. *Oncotarget*. pp. 33122,33131.

Wang, M. et al., 2009. Pigment epithelium-derived factor suppresses adipogenesis via inhibition of the MAPK/ERK pathway in 3T3-L1 preadipocytes. *AJP: Endocrinology and Metabolism.* pp. E1378, E1381-E1386.

Xu, Z. et al., 2019. Elucidating the Regulatory Role of Melatonin in Brown, White, and Beige Adipocytes. *Advances in nutrition*. pp. 1-2. Available at: https://www.ncbi.nlm.nih.gov/pubmed/31355852. [Accessed July 20. 2019].

Yoshida, K. et al., 2019. Monoacylglycerol lipase deficiency affects diet-induced obesity, fat absorption, and feeding behavior in CB_1 cannabinoid receptor-deficient mice. *The FASEB Journal*. p. 1.

Zechner, R. et al., 2005. Lipolysis: pathway under construction. *Current Opinion in Lipidology.* p. 337.

Zechner, R. et al., 2009. Adipose triglyceride lipase and the lipolytic catabolism of cellular fat stores. *Journal of Lipid Research*. p. 6.

Zimmermann, zR. et al., 2009. Fate of fat: The role of adipose triglyceride lipase in lipolysis *Biochimica et Biophysica Acta-Molecular and Cell Biology of Lipids*. pp. 494-496.